

Department of Electrical and Computer Systems Engineering

Technical Report MECSE-3-2005

DWDM Advanced Optical Communication-Simulink Models: Part
I-Optical Spectra

L.N Binh and Y.L. Cheung

MONASH
UNIVERSITY

DWDM ADVANCED OPTICAL COMMUNICATIONS – SIMULINK MODELS: PART I – OPTICAL SPECTRA OF RZ-NRZ-ASK MODULATION FORMATS

L.N Binh and Y..L. Cheung

Department of Electrical and Computer Systems Engineering, Monash University

Clayton, Victoria 3168 Australia

e-mail: le.nguyen.binh@eng.monash.edu.au

Summary

The transmission of DWDM channels over ultra-long distance with minimum impairments is very critical in modern optical networks. In this reports we propose a modeling platform MATLAB SIMULINK for optical transmission, the optically amplified DWDM optical transmission system. We briefly introduce the fundamentals understandings of optical fibers, digital communications systems, fiber propagation effects, sources and multiplexers, de-multiplexers etc. that influence the transmission of optical carrier modulated signals, such as chromatic dispersion, polarization dispersion and non-linear phase-induced effects etc. Further the report aims to develop the model as an efficient laboratory teaching tool in advanced optical communications systems for postgraduate studies.

The development of 10 Gb/s DWDM optical fiber communication system has been successfully completed developed based on a prototype through the MATLAB SIMULINK platform R14 partitioned into a number of Parts. In this report, the Part I of the series, different modulation formats such as RZ, CSRZ, RZ-DPSK and Chirped NRZ are modeled. Other modulation formats have also been investigated such as the single-side band, DSB modulation are modeled. Photonic components such as dispersion compensating modules (DCM), optical amplifiers (power booster, in-line and pre-amplifying EDFAs are developed. Their SIMULINK models are reported in the series. The propagation model of the

1-1

optical fiber, in the linear domain, as a low pass filter is presented by the Z-transform. Finally the integration of all these modulation formats and formats, system photonic components and the fiber propagation is performed.

This document is the first part of a series, demonstrates the optical spectra of RZ and NRZ ASK modulation formats. Experimental demonstration of the spectra is also given. Various modulation formats of baseband and sideband signal band pulse profile of Gaussian and, raised cosine profiles are described. Optical multiplexers and de-multiplexers have been implemented for 16 and/or 32 channels with 100 GHz, 200 GHz channel spacing leading to multi Tera-bits/sec capacity system.

An integrated development system of a number of sub-system developments using MATLAB SIMULINK will be demonstrated at later stages. Procedures for setting up required simulation inputs and scopes for monitoring and extracting of simulated results are included in the Appendix.

TABLE OF CONTENTS

Summary	1-1
1 Introduction	1-7
2 Modulation Techniques in DWDM optical transmission systems	2-8
2.1 Optical Transmission Systems: Introductory Remarks	2-8
2.2 NRZ and RZ OOK/ASK Data Formats	2-10
2.2.1 ASK Modulation	2-11
2.2.3 Single Drive Interferometric Modulators	2-11
2.2.4 SSB modulation	2-12
2.2.5 Dual Electrode MZIM	2-13
2.3 Pulse Profile	2-13
2.4 WDM	2-15
2.5 Frequency Scaling	2-16
2.6 Random Binary Data (PRBS) Stream	2-17
3 SIMULATORS	3-17
3.1 NRZ and RZ ASK Modulation Simulator	3-17
3.2 Pulse profile simulator sub-system	3-19
3.2.1 Gaussian profile	3-19
3.2.2 Raised cosine profile	3-21
4 WDM channels	4-24
4.1 RZ- format demodulation	4-30
5 Dual electrode MZ Modulator: Simulation and Experimental Results	5-32
5.1 Dual electrode MZ Modulator DSB Simulation	5-32
5.2 DSB Carrier Suppressed (DSB-CS) modulation using dual drive MZIM	5-34
5.3 SSB Simulation	5-36
5.4 Modulation formats Experiments: Single, Cascade and Dual electrode MZIM	5-38
5.5 Dual electrode MZ Modulator SSB Simulation	5-44
5.6 Hilbert Transform SSB MZ Modulator Simulation	5-46
5.7 SSB Demodulator Simulation	5-49
6 Concluding Remarks and Further Development	6-51
6.1 Further Development	6-51
6.2 Remarks	6-51
	1-3

7	References.....	7-52
8	Appendix.....	8-52
8.1	Simulation Requirement	8-52
8.2	Initialization	8-53
8.3	Simulation Block Specification	8-53
8.3.1	FFT Spectrum Scope.....	8-53
8.3.2	Zero-Order Hold	8-54
8.3.3	Phase Modulation.....	8-55
8.3.4	S-Function.....	8-55
8.3.5	Digital Filter Design	8-56
8.3.6	Time Eye Diagram Scope	8-57

TABLE INDEX

Table 1:	Dual Drive MZ SSB Modulator experimental parameters	5-41
Table 2:	The system scaled frequencies following ITUT standard	8-59

TABLE OF FIGURES

<i>Figure 1: DWDM fiber optic communication system (a) long haul optically amplified spans with inline optical regenerators and (b) optical spectra of DWDM channels.</i>	2-10
<i>Figure 2: Binary RZ and NRZ signal formats</i>	2-11
<i>Figure 3: A schematic diagram of a Mach-Zehnder modulator in the OFF state[2] with the total phase variation in one path of 180°</i>	2-12
<i>Figure 4: A block diagram of a Dual electrode MZ modulator</i>	2-13
<i>Figure 5: Raised cosine filter shape with different roll-off factors $0 < \alpha < 1$</i>	2-15
<i>Figure 6 (a) Single spectrum consists of 2 channels wavelength in Multiplexer (b) Two different wavelength signal spectra after a de-multiplexer</i>	2-16
<i>Figure 7: Transfer characteristic of external modulator.</i>	2-17
<i>Figure 8: SIMULINK model of modulating data stream PRBS with random NRZ signal at 10 Gb/s.....</i>	3-18
<i>Figure 9: RZ signal generation SIMULINK platform</i>	3-18
<i>Figure 10(a) Random NRZ ASK signals (b) RZ binary random sequence and (c) RZ binary eye diagram of the input stream</i>	3-19
<i>Figure 11 Spectrum of (a) NRZ and (b) RZ modulated lightwave signals</i>	3-19
<i>Figure 12: SIMULINK model for generation of modulation of Gaussian data sequence at 10 Gb/s.....</i>	3-20
<i>Figure 13: Eye Diagram of Gaussian RZ signal PRBS random sequence.</i>	3-21
<i>Figure 14: (a) Spectrum of NRZ Gaussian random PRBS data (b) Gaussian profile baseband spectrum and (c) Spectrum of optically modulated Gaussian PRBS sequence.....</i>	3-21
	1-4

Figure 15: SIMULINK model for the modulation of raised cosine NRZ PRBS.	3-22
Figure 16: (a) Spectrum of raised cosine NRZ format lightwaves at base band (b) Spectrum of the raised cosine modulated lightwaves (c) Demultiplexed spectrum of the raised cosine modulation lightwave channel, back to back test (d) Spectrum of demodulated raised cosine PRBS.	3-23
Figure 17: Demodulated sequence of raised cosine pulses (b) Eye diagram of the NRZ raised cosine PRBS at the transmitter and (c) Eye Diagram of the raised cosine pulse sequence, error free at BER = 10^{-12}	3-24
Figure 18: Multiplexer (MUX) block diagram	4-24
Figure 19: De-multiplexer (Demux) block diagram	4-25
Figure 20: 16 channels Simulink Platform	4-25
Figure 21: The Block Properties of PM modulator.	4-27
Figure 22 Block diagram of the external MZIM.....	4-28
Figure 23 Gaussian shaped modulating channel input of the Simulator.	4-28
Figure 24 Carrier frequency, phase modulated signal and MZIM output time-dependent signal.	4-29
Figure 25 Spectrum of (a) a Gaussian-shaped data stream at 192.1THz (5.7THz represents) Input signal with 200GHz and (b) 16 multiplexed channels of 200 GHz channel spacing.	4-30
Figure 26 (a) The first 16 channels spectrum signal in 32 channels platform (b)The second 16 multiplexed channels and (c) Spectrum of a de-multiplexed channel 1 192.1THz (5.7THz is the scaled down centre frequency) in passband.	4-30
Figure 27: Demodulation Simulink Platform	4-31
Figure 28 (a) Spectrum of the de-modulated RZ-ASK data stream (b) de-modulated output signal (10Gb/s Gaussian shaped) (c) Eye diagram of the de-modulated output signal (10Gbps Gaussian shaped) - $Q= 7$, BER 10^{-12}	4-31
Figure 29: (a) RZ Gaussian pulse shaped demodulated signal spectrum using high resolution sampling (b) RZ Gaussian pulse shaped eye diagram signal at the output of the demodulator.	4-32
Figure 30: Dual electrode MZ DSB Modulator	5-33
Figure 31: (a) Upper Arm of Dual electrode MZ modulator $\cos(\omega_c t + \gamma\pi + \alpha\pi \cos\omega_m t)$ (b) Lower Arm of Dual electrode MZ modulator $\cos(\omega_c t + \alpha\pi \cos\omega_m t + \theta)$ and (c) Dual Electrode MZ modulator DSB output spectrum.....	5-34
Figure 32 Simulink model of the dual-drive DSB MZIM.....	5-35
Figure 33 Dual Electrode MZ modulator DSB CS spectrum result	5-36
Figure 34 Simulink sub-System for Single Side band Modulation	5-37
Figure 35 (a) Upper modulation arm signals: $\sin\omega_m t * \sin \omega_c t$ (b) Lower Modulation arm signals: $\cos\omega_m t * \cos \omega_c t$	5-38
Figure 36 (a) Upper and lower sideband spectrum at the upper arm (b) Upper and lower sideband spectrum at the lower arm and (c) SSB signal spectrum without Carrier. 5-38	
Figure 37 Dual-Drive MZIM Experiment Set-up.	5-39

Figure 38: Schematic Diagram of the Dual-Drive MZ Modulator Experiment Set-Up.	5-39
Figure 39: (a) Positive (b) negative Transfer Characteristic Curve of Dual Drive MZIM dual-bias.	5-40
Figure 40 Output of the dual-drive MZ SSB modulator at 1550.44nm with (a) lower SSB (b) Upper SSB	5-41
Figure 41 Dual Drive MZ SSB Modulator Output Signal Power of 0.5dBm, without optical preamp.	5-42
Figure 42 40 b/s optical modulation system set-up back to back with optical filters, optical amplifiers and MUXES and DEMUXES.	5-43
Figure 43 Optical spectra CS-RZ, NRZ and RZ at 40 Gb/s.....	5-43
Figure 44 BER versus received optical power (at the power meter – 1;10 coupler before Rx). Legends: “blue” CSRZ-DPSK (one NELAWG); “red” – RZ DPSK(one NELAWG); “green” NRZ ASK(one NELAWG); “yellow” – CSRZ- ASK (one NELAWG); “c” RZ-ASK(one NELAWG); Note: only one optical filter NEL AWG is used; “Red o” CSRZ DPSK TWO AWGs used; “blue o” RZ-DPSK TWO AWGs used. Note: the DPSK formats will be reported in a future document.	5-44
Figure 45: Phase characteristic curve to determinate bias points of two arms in dual drive MZ modulator	5-45
Figure 46: Dual Drive SSB MZ modulator platform.....	5-45
Figure 47: (a) Upper Arm of Dual electrode MZ modulator $\cos(\omega_c t + \gamma_1 \pi + \alpha \pi \cos(\omega_{rf} t + \theta_1))$ and (b) Lower Arm of Dual electrode MZ modulator $\cos(\omega_c t + \gamma_2 \pi + \alpha \pi \cos(\omega_{rf} t + \theta_2))$ and (c) Dual Electrode MZ modulator SSB system spectrum result with the cancellation of the upper SB (d) resultant spectrum with lower SB cancelled out	5-46
Figure 48: SSB Hilbert transform phase shift modulator.....	5-47
Figure 49: (a) Input RF signal time scope (cosine signal) (b) Hilbert transform the input RF signal $H\{x(t)\} = A \cos(2\pi f_o t - \pi/2) = A \sin((2\pi f_o t))$	5-48
Figure 50: Upper arm of dual electrode MZ modulator with delay 10ns in Hilbert transform phase shift system (b) Lower arm of dual electrode MZ modulator with Hilbert transform phase shift $\theta = \pi/2$ and (c) Dual electrode MZ modulator SSB system spectrum result with lower SB cancels out.....	5-48
Figure 51: SSB Demodulation sub-Simulator.	5-50
Figure 52: Demodulate f_c carrier time scope (b) Demodulate cosine signal time scope before LPF(c) Demodulate signal time scope after LPF.....	5-50
Figure 53: (a) Demodulated signal spectrum and (b) Demodulated signal Eye Diagram has $Q = 8$ and and $BER = 10^{-15}$	5-50
Figure 54: The block diagram of receiver[2].....	6-51
Figure 55 Spectrum Scope Specification	8-54
Figure 56: Zero-Hold Order Specification.....	8-55
Figure 57 Phase Modulation block specification	8-55
Figure 58: Digital Filter Specification	8-57
Figure 59 Eye diagram specification.....	8-58
	1-6

1 Introduction

Optical fibers are now installed throughout global and terrestrial networks as the transmission media of ultra-long distance communication backbones. In order to upgrade and respond to the Internet demands of information capacity, several optical-carrier modulated channels are multiplexed and transmitted over a single single-mode fiber, now commonly termed as the wavelength division multiplexed (WDM) optical communications. When the frequency spacing between WDM channels are narrow, in order of 50- 100 GHz or lower, the number of channels becomes dense and we hence DWDM (D stands for dense).

When modulated signals are transmitted over a long reach fiber at high bit rate, they suffer loss and pulse broadening. These impairments would be compensated by dispersion compensators and optical amplifiers. However as the bit rate is increased, especially at 40 Gb/s or higher the limitations and novel modulation techniques can be used to reduce the signal band width and increase the total power distributed over the whole signal band. The role of modulation formats in advanced optical fiber communications has recently attracted attention for high spectral efficient transmission. This report thus addresses a new modeling platform developed under Matlab™ SIMULINK for several important modulation techniques for optical channels and their transmission over long distance optical spans.

This report is the Part I of the series of novel models based on Matlab™ SIMULINK simulation platform for DWDM Advanced Modulation Optical Fiber Transmission Systems. It focuses on the modulation techniques and spectral properties. Experimental results are also demonstrated. NRZ binary data stream PRBS is constructed with pulse shapes of Gaussian and raised cosine profiles. External optical modulators MZIM are used throughout as the modulation device(s) for transmitters either in single drive or dual

drive modes in single stand alone or in cascaded pair to generate amplitude, phase or frequency modulation formats.

The fiber dispersion effects, both chromatic and polarization mode dispersion (PMD), nonlinear phase dispersion and attenuation are briefly given. Compensators are introduced in separate parts including EDF amplifiers, Raman optical amplifiers and dispersion compensators. Optical multiplexers, de-multiplexers and photonic demodulators are also employed. These are reported in the next part of the series.

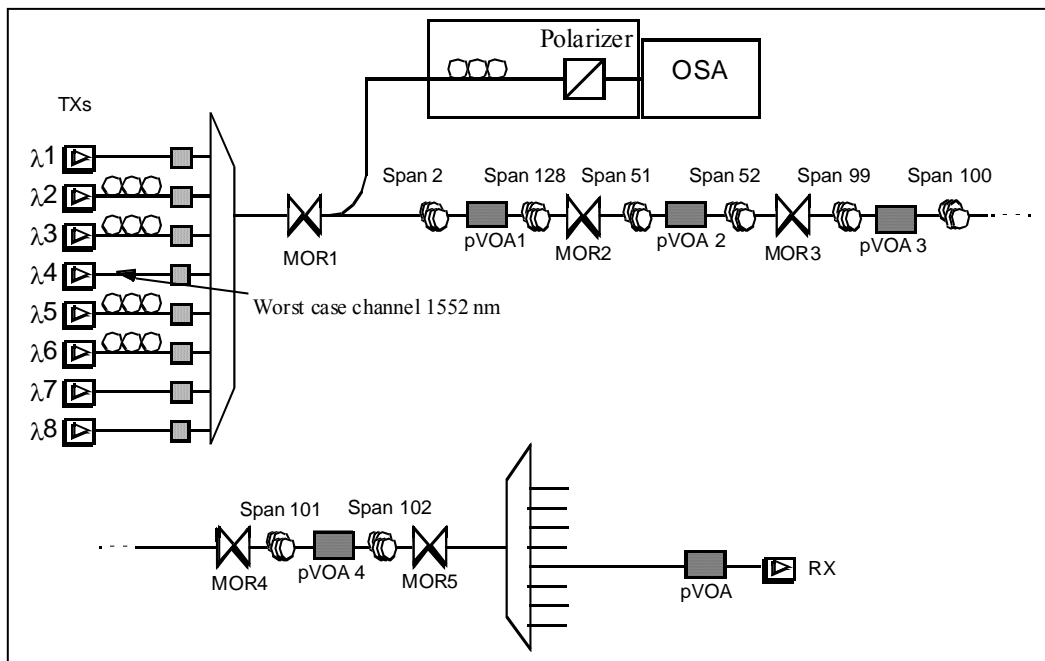
Different formats of modulation are developed such as NRZ-ASK, RZ-ASK, CSRZ, RZ-DPSK, and NRZ-DPSK for Gaussian and raised cosine pulse profile. Single or double sidebands modulation formats spectra are generated using dual electrode MZ modulators can be. Analytical, simulated and experimental optical frequency spectra have been obtained and confirmed. Single and dual electrode driven MZIMs can be employed to generate modulation formats. SSB modulation experiment is also performed and confirmed with the simulated outputs under SIMULINK.

The model is also integrated with other SIMULINK models to simulate signal propagation through optical communication simulation systems. These models will be reported in the next parts of the series. This report is organized as follows: In Section 2 an introductory remarks of the optical communication system and advanced modulation techniques for optical fiber communications systems. Details of optical components of the transmission system especially the optical transmitter and the modulation technique are elaborated. Section 3 describes the pulse shape profile, the spectra and the corresponding Simulink simulation models and results. Section 4 reports the muxed channels and the use dual electrode MZ modulator for single sideband generation. Experimental and simulation results are given. Finally concluding remarks are stated and linked to other parts of the series.

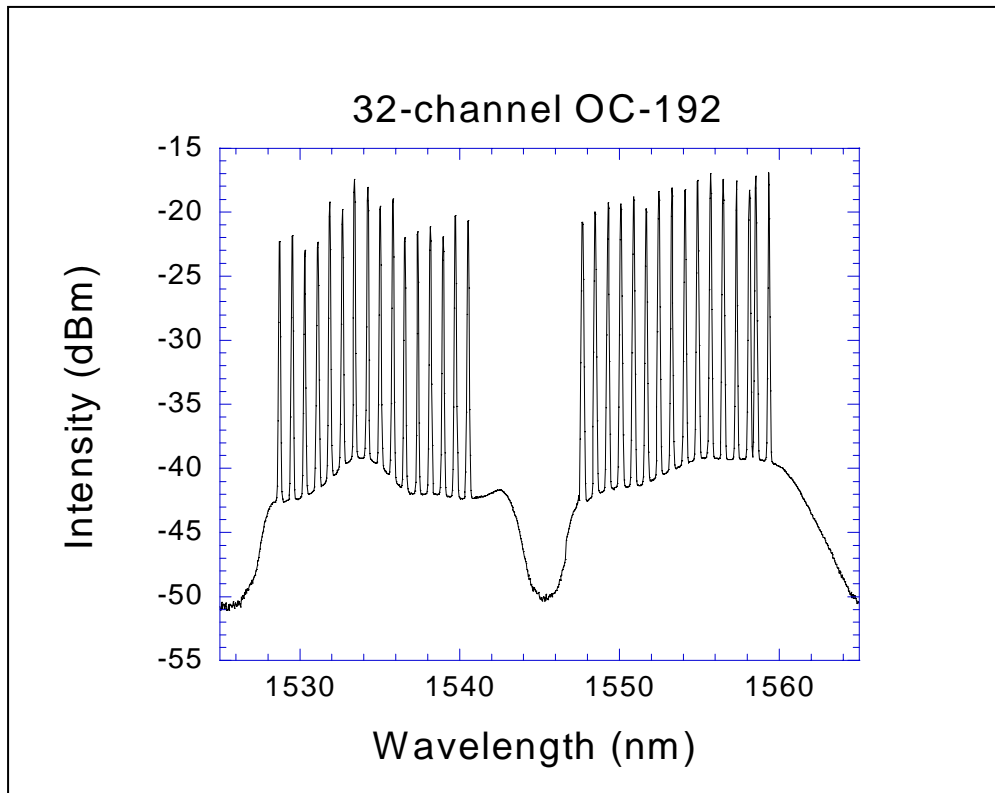
2 Modulation Techniques in DWDM optical transmission systems

2.1 Optical Transmission Systems: Introductory Remarks

The optical communication system is becoming a popular transmission media as it has several advantages, such as enormous bandwidth, low loss rate, electrical isolation, no electromagnetic interference, lower cost per bit, reliability and security. The structure of an advanced optical communication system is shown in Figure 1 in which lightwaves can be generated and directly modulated from a laser source or eternally modulated by an electro-optic or electro-absorption modulator. These modulated lightwaves are then transmitted a single mode optical fiber either of standard or non-zero-dispersion shifted (NZDSF) types and compensating fibers. The photonic channels are then optically amplified to compensate for the propagation losses through fibers and other photonic components. Several spans of distance in order of 80 km to 120 km are cascaded to for ultra-long haul optical transmission systems.



(a)



(b)

Figure 1: DWDM fiber optic communication system (a) long haul optically amplified spans with inline optical regenerators and (b) optical spectra of DWDM channels.

The optical channels are then demultiplexed and detected with additional mopping of dispersion (chromatic and polarization) if necessary and optical amplification with provision of attenuators. They are then regenerated or received in the electronic domain.

2.2 NRZ and RZ OOK/ASK Data Formats

The Non-Return to Zero (NRZ) format is a normal and commonly used pulse coding modulation format in optical communication systems as shown in Figure 2. This format is sending a signal during the bit period for a '1' and null signal during a '0'. NRZ has potential pulse spreading problems. It also does not efficiency on using bandwidth. The Return to zero (RZ) of Figure 2 has half of the bit period for a '1' when the pulse signal is

2-10

high and null signal for a '0' and is more tolerant towards pulse dispersion. The bandwidth required by RZ is twice larger than that of NRZ; therefore it only requires half of NRZ power in transmission.

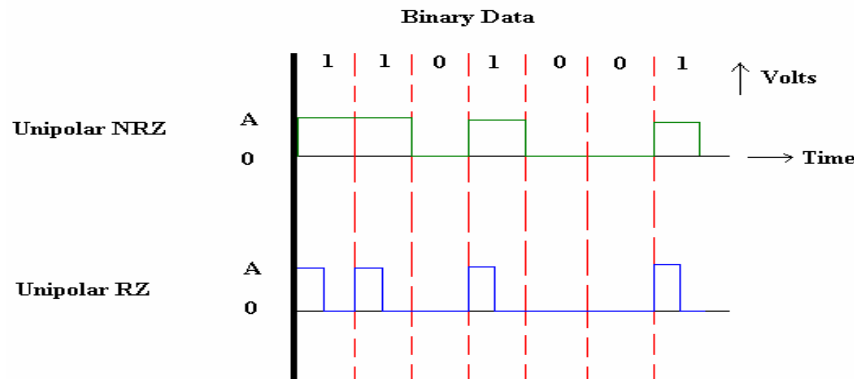


Figure 2: Binary RZ and NRZ signal formats

2.2.1 ASK Modulation

The random binary data is a binary data signal in which the pulse is either 1 or 0 shaped (like square wave). However this random binary pulses data requires a wider bandwidth. It is used to modulate the carrier signal. Amplitude Shift Keying (ASK) is a well known modulation technique that allows digital signal $m(t)$ multiply with a carrier wave f_c . It can be mathematically defined by

$$s(t) = Am(t) \cos 2\pi f_c t, \quad \text{for } 0 < t < T \quad (1)$$

where A is an amplitude envelop, $m(t)$ is the binary signal state of “1 or 0”, f_c is the optical carrier frequency and T is the bit period. The frequency spectrum of an ASK signal can be represented by the baseband spectrum of the modulation $m(t)$ but shifted to the carrier frequency f_c .

2.2.3 Single Drive Interferometric Modulators

Modern optical communication systems employ two types of external modulators for ASK modulation formats, the interferometric or electro-absorption (EA) types. However

the most popular one is the LiNbO₃ MZIM waveguide modulator configuration because of its low optical loss and high electro-optic coefficient while the EA semiconductor waveguide modulator does not offer the flexibility in modulation and linearity[1].

The structure of the single drive MZIM is shown in *Figure 3* in which the incoming lightwaves is equally split into the two waveguide arms forming an optical inteferometer. An external voltage is applied onto one electrode generating a change in the refractive index of the optical waveguide branch via the electro-optic effect. Depending on the orientation of the crystal substrate chirp or chirp free optical modulation can be achieved. For lithium niobate the X-cut Z-propagating is usually preferred to obtain chirp free modulation.

When a phase difference between two optical arms is 180 degree the lightwave paths combine destructively and hence the output is at its minimum point or “0-state”. When the lightwaves from the upper and lower arms recombine at the output of MZI modulator, if the carriers of two arms are in phase, a maximum constructively output is formed.

In the case of dual electrode drive, voltages can be applied to both paths and hence one could inject a phase bias to generate either double or SSB property of the lightwaves in the frequency domain.

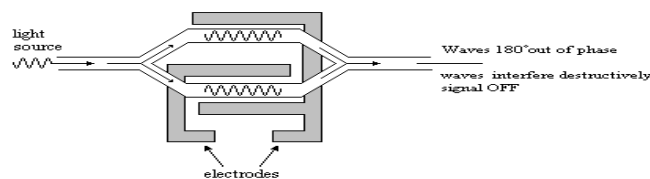


Figure 3: A schematic diagram of a Mach-Zehnder modulator in the OFF state[2] with the total phase variation in one path of 180°.

2.2.4 SSB modulation

Fiber chromatic dispersion accumulates along the fiber propagation path. Thence pulse spreading is influence by the sideband spectrum components of the modulated signals. Therefore a reduction of the total bandwidth of a carrier modulated wideband signals is

2-12

critical. In addition, with DSB transmission system, the data signals contained in the upper sideband is identical to the information contained in the lower sideband. Thence in order to minimize the effects of the fiber chromatic dispersion and to increase the optical bandwidth efficiency, the optical SSB modulation can be used[3] provided that complexity in implementation at ultra-speed operation is not the constraint.

2.2.5 Dual Electrode MZIM

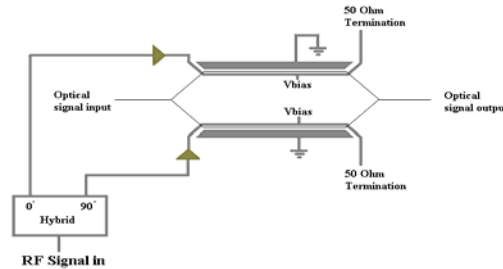


Figure 4: A block diagram of a dual electrode MZ modulator

A dual electrode MZI modulator is shown in Figure 4 in which the RF signals are applied to both of the two electrodes with a $\pi/2$ phase shift using a hybrid 90o splitter to generate SSB signal. In order to generate DSB signal, both of the arms are biased at either minimum or maximum transmission points depending on whether a carrier-suppress (CS) is used as similar to the case of single electrode MZ modulator. For DSB carrier suppress (CS), one of the arm applied $-\pi/2$ while another arm applied $\pi/2$. Carrier suppress modulation can save the power transmission and rejections of intersymbol interference (ISI) with adjacent symbols.

The bias of the electrodes, either at maximum, minimum or quadrature points, is very critical for the operation of amplitude or phase dependent modulation and carrier suppression or carrier max, for example the RZ-ASK, NRZ-ASK or CSRZ, CS-NRZ or RZ-DPSK, NRZ-DPSK etc.

2.3 Pulse Profile

The random binary pulses data requires a full bandwidth and hence the complexity in the contraction of the transmitters at ultra-high speed and pulse spreading problems. It is normally preferred to create a pulse profile that conveys the same data signal by using smaller bandwidths. This offers an advantage in reduction of inter-symbol interference (ISI). Pulse shapes can be Gaussian, raised cosine, half sinusoid or quadrature partial. In this project, Gaussian shaped and raised cosine filter pulse shapes are employed as they are usually the shapes of the modulated lightwaves at the output of the MZIM.

2.2.6.1 Gaussian Pulse Shaping

A Gaussian pulse shape replaces the binary signal data with a Gaussian pulse. It minimizes the harmonics problem of square pulse signal. Furthermore due to the parabolic transfer characteristics of the MZIM the Gaussian or raised cosine profiles are much more realistic than the rectangular pulse shape. AS normal the Gaussian pulse can be expressed as

$$\text{Gaussian pulse} = e^{-(t/\tau)^2} \quad (2)$$

2.2.6.2 Raised-Cosine Pulse Shaping

A raised cosine filter can be introduced so as to minimize the bandwidth by low passing the binary signal. This is modeled in Simulink as the output PRBS of the filter with input PRBS rectangular pulse sequence. A raised cosine filter is a LPF commonly used in transmission system for pulse shaping than Gaussian pulse shaping. This shape offers low harmonic distortion than that of Gaussian shaping. The raised cosine pulse shape has some built in flexibility characteristics, which can be adjusted from the minimum Nyquist bandwidth, $W/2$ (*sinc* pulse) to W (pure square/rectangular pulse). The roll off factor alpha ($0 < \alpha < 1$) is used to govern the bandwidth as shown in Figure 5. The raised cosine pulse in time domain [4] can be expressed as:

$$p(t) = \begin{cases} 1 & |t| < (1-\alpha)\frac{T}{2} \\ \frac{1}{2} \left[1 - \sin \left(\frac{\pi \left(|t| - \frac{T}{2} \right)}{\alpha T} \right) \right] & (1+\alpha)\frac{T}{2} \geq |t| \geq (1-\alpha)\frac{T}{2} \\ 0 & |t| > (1+\alpha)\frac{T}{2} \end{cases} \quad (3)$$

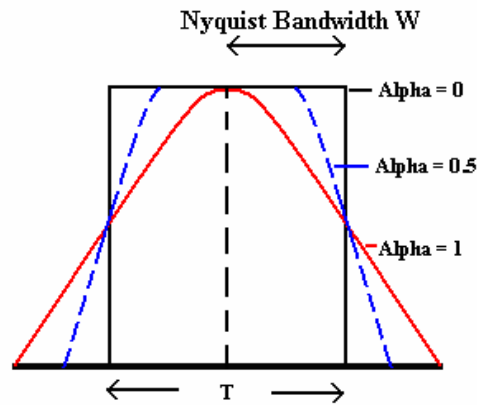


Figure 5: Raised cosine filter shape with different roll-off factors $0 < \alpha < 1$

2.4 WDM

Wavelength Division Multiplexing (WDM) couple sources and emit at different wavelengths into the single mode optical fiber and each channel has different wavelength which avoids cross-talk when they are de-multiplexed at the receiving end. Individual wavelength channels are multiplexed into the single mode fiber, thus all channels have their own full bandwidth. At the output of the optical fiber, the optical signals are then de-multiplexed by the receiver which can separate the various carrier wavelengths and the optical signal will be recovered to its original modulating signal from modulated carrier at the demodulator.

The difference between WDM and Dense WDM is the wavelength spacing between channels. The capacity in DWDM is greater than WDM provided that optical muxes and demuxes can offer the required bandwidth and integrity of signals passing through them.

In DWDM system, a multiplexer combines various optical wavelength lightwaves from multiple channels laser operating in the CW mode and converges them into one directional output as shown in Figure 6.

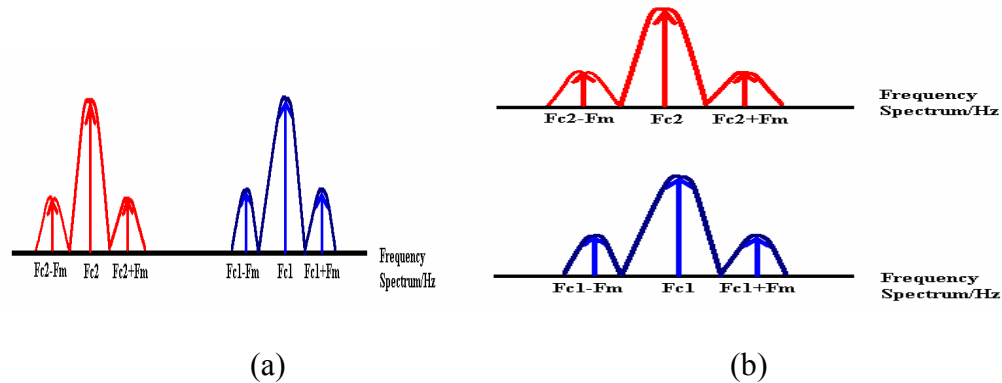


Figure 6 (a) Single spectrum consists of 2 channels wavelength in Multiplexer (b) Two different wavelength signal spectra after a de-multiplexer

A de-multiplexer is at the receiving end of DWDM system to filter out the each channels' different wavelength signal and to couple them into different channels output as shown in **Figure 6(b)**.

2.5 Frequency Scaling

The frequency of whole photonic system is required to be scale down because the carrier frequency and the data stream signal have a large scale difference. For example, if the carrier frequency is 1550nm (corresponding to a frequency of 1.935×10^{14} Hz), while the modulating signal is 10GHz. Due to this ultra-high carrier frequency, there are approximately 19350 light wave pulses in one 10Gb/s data signal pulse. It is very difficult to display on the sampling scope of SIMULINK as the optical and modulation frequencies are so close[5]. In addition, for DWDM channels, the system requires very high sampling frequency to cover the highest and the lowest spectral range which can be several THz. Therefore, other frequency bands can be used to represent DWDM channels

in the C- or L- band frequencies. Following the ITU-T standard, the scaled frequencies are showed in Table 2 given in the Appendix.

2.6 Random Binary Data (PRBS) Stream

There is a random data stream box in which the data output rate is set at a data rate of 10 Gb/s or 40 Gb/s. The DC bias and the constant input is the transfer characteristic setting. This is artificial DC bias input data. The bias voltage changes the refractive index by electro-optic effect. The external modulator can be biased in the linear range at minimum, phase quadrature or maximum transmission regions as shown in Figure 7.

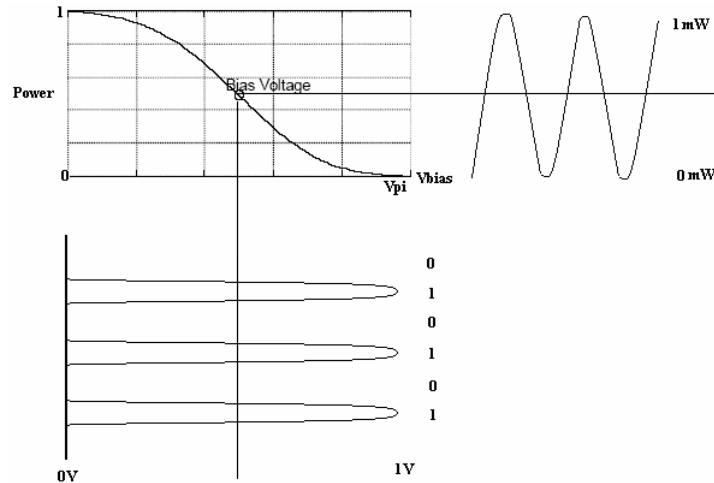


Figure 7: Transfer characteristic of external modulator and the corresponding input and output signals.

3 SIMULATORS

3.1 NRZ and RZ ASK Modulation Simulator

Modulating Data Stream with Random Binary Data Stream in 10Gbps

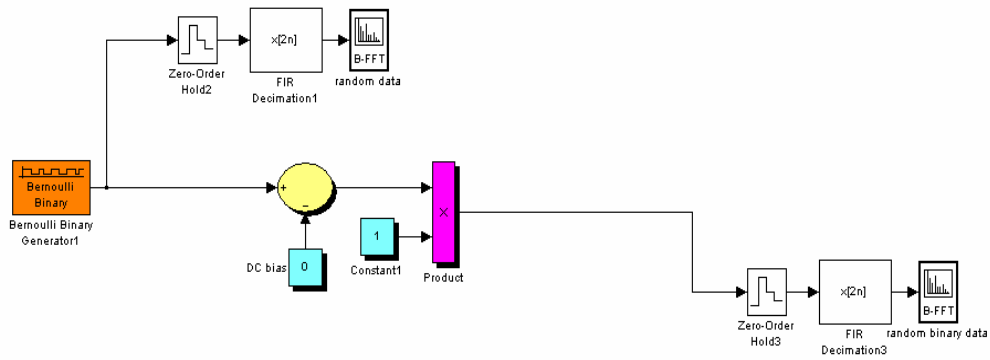


Figure 8: SIMULINK model of modulating data sequence PRBS with random NRZ signal at 10 Gb/s

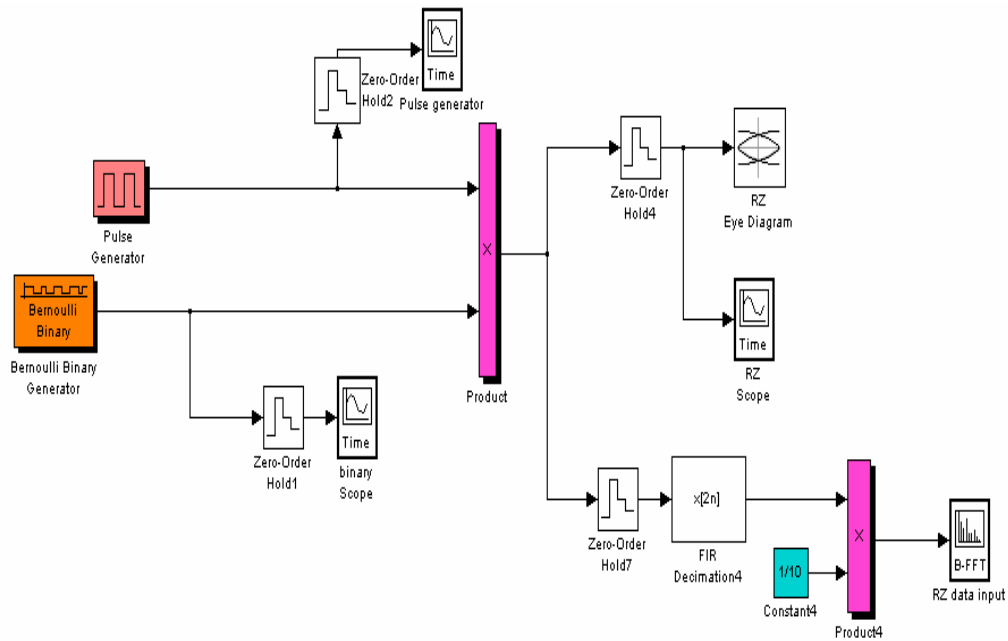


Figure 9: RZ signal PRBS generation SIMULINK platform

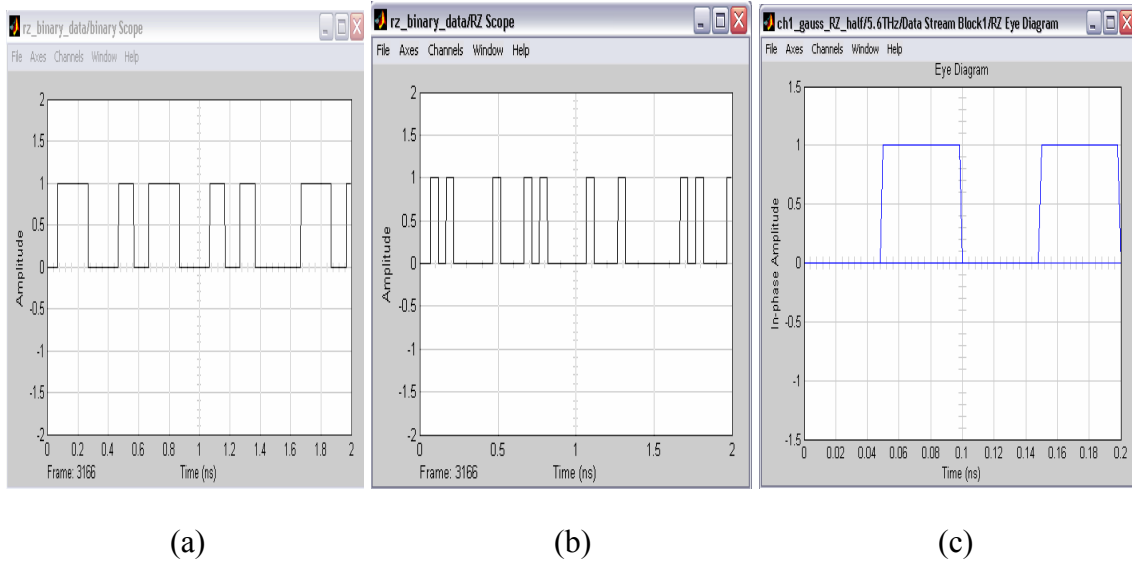


Figure 10(a) Random NRZ ASK signals (b) RZ binary random sequence and (c) RZ binary eye diagram of the input stream

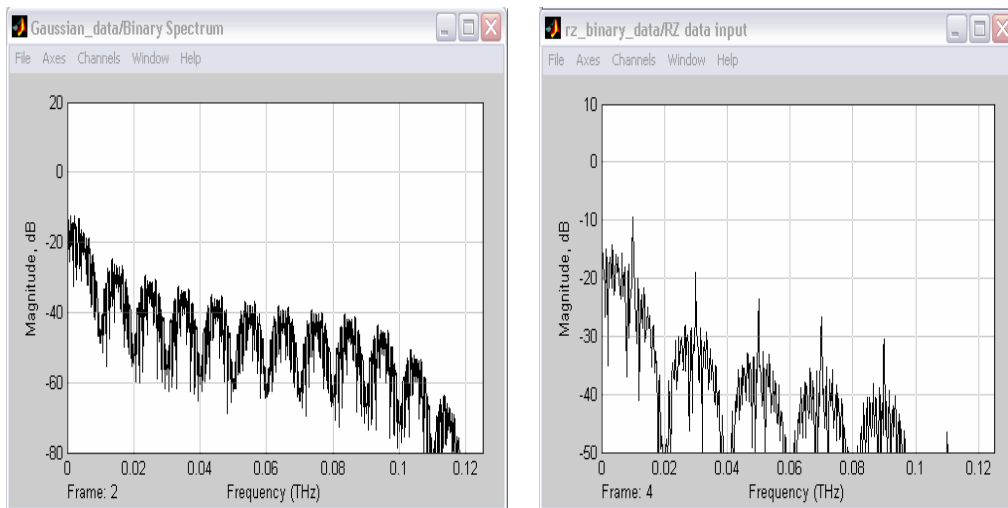


Figure 11 Spectrum of (a) NRZ and (b) RZ modulated lightwave signals

3.2 Pulse profile simulator sub-system

3.2.1 Gaussian profile

A Gaussian pulse shape replaces the binary signal data with a Gaussian pulse.

$$\text{Gaussian pulse} = e^{-(t/\tau)^2} \quad (4)$$

The signal now is then given by

$$u(t) e^{-(t/\tau)^2} \quad (5)$$

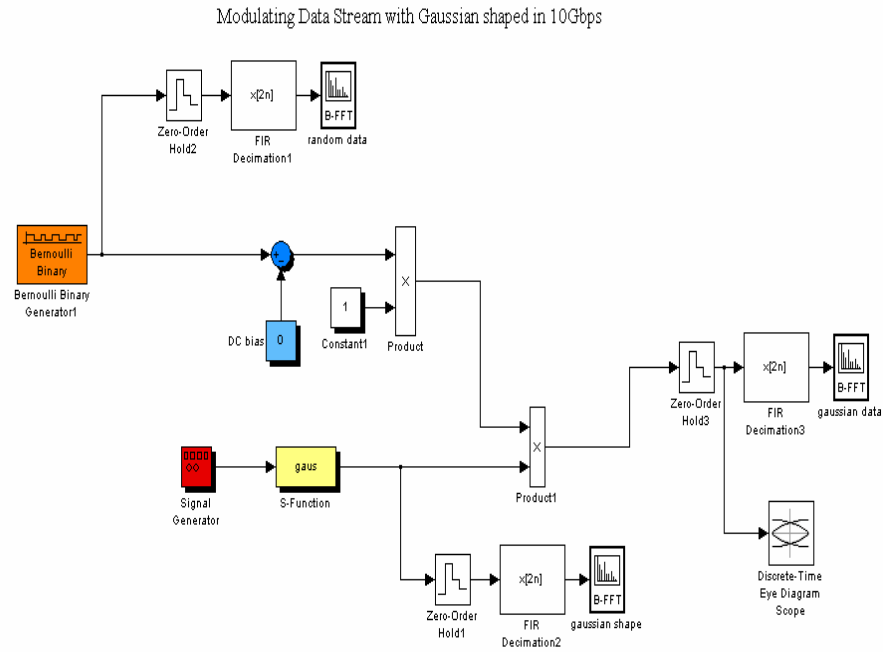


Figure 12: SIMULINK model for generation of modulation of Gaussian data sequence at 10 Gb/s.

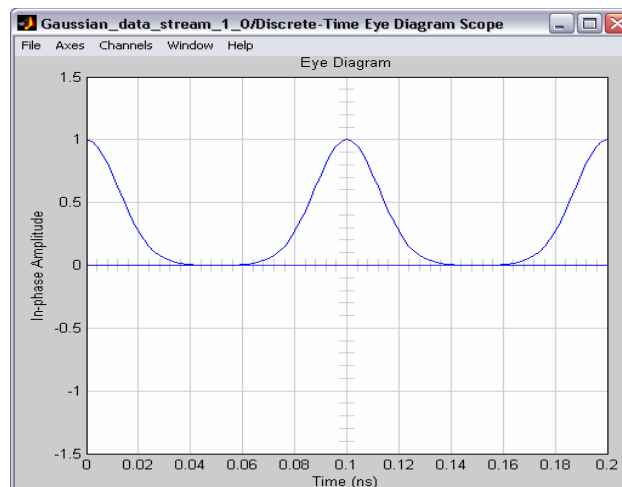
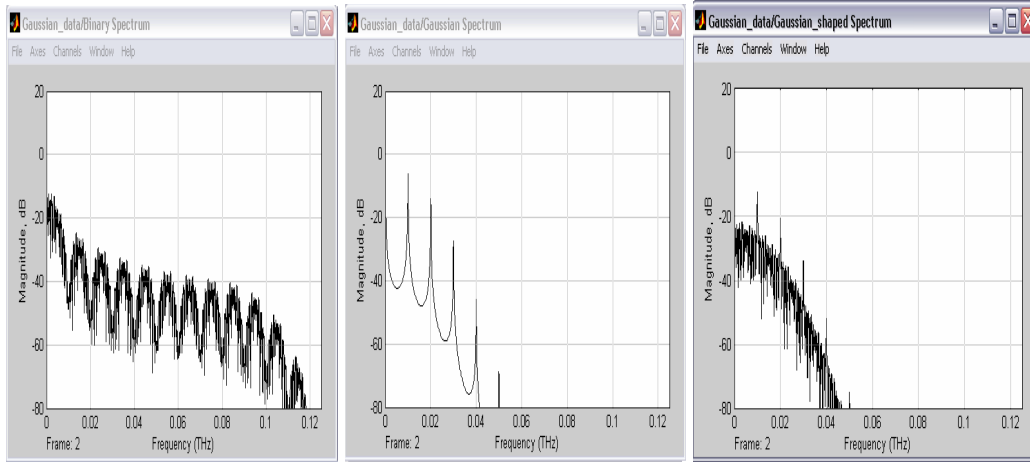


Figure 13: Eye Diagram of Gaussian RZ signal PRBS random sequence.



(a)

(b)

(c)

Figure 14: (a) Spectrum of NRZ Gaussian random PRBS data (b) Gaussian profile baseband spectrum and (c) Spectrum of optically modulated Gaussian PRBS sequence.

3.2.2 Raised cosine profile

The input random binary signal is in time domain in this system. We use the raised cosine filter to reduce the signal bandwidth and the raised cosine pulse in time domain[4] is:

$$p(t) = \begin{cases} 1 & |t| < (1-\beta)\frac{T}{2} \\ \frac{1}{2} \left[1 - \sin \left(\frac{\pi \left(|t| - \frac{T}{2} \right)}{\beta T} \right) \right] & (1+\beta)\frac{T}{2} \geq |t| \geq (1-\beta)\frac{T}{2} \\ 0 & |t| > (1+\beta)\frac{T}{2} \end{cases} \quad (6)$$

Modulating Data Stream with Raised Cosine Filter in 10Gbps

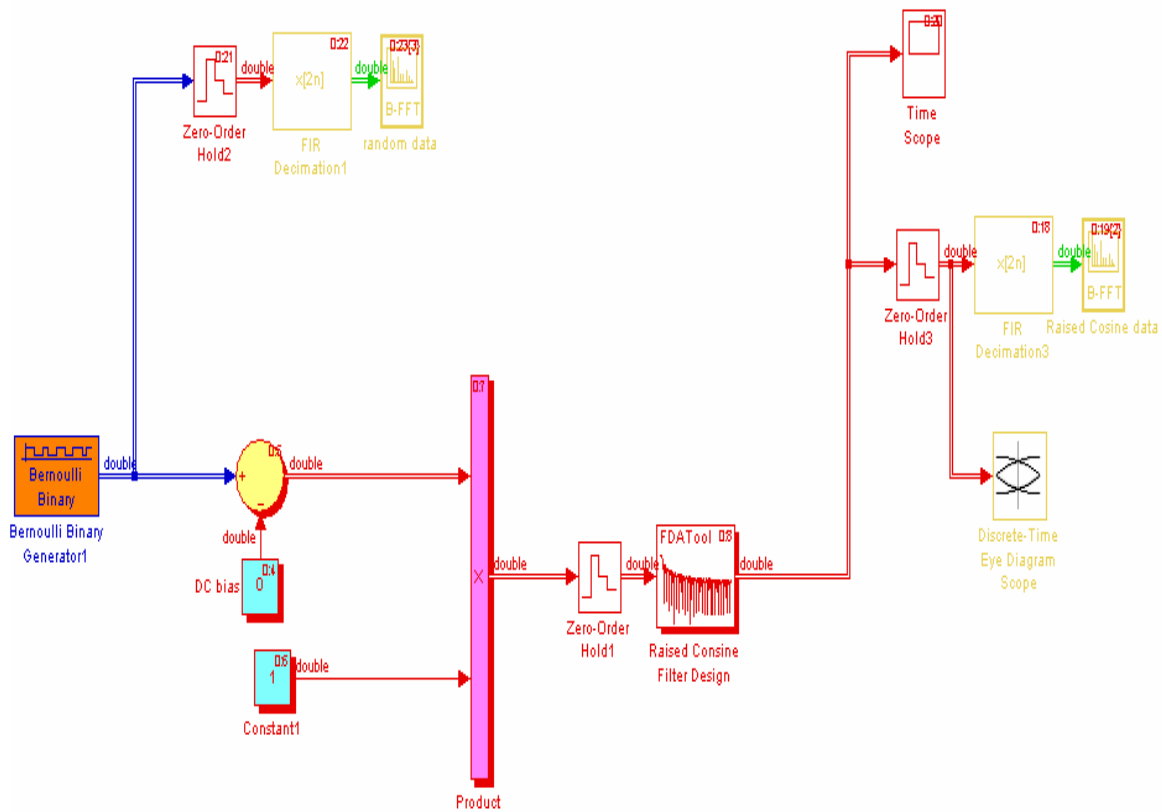
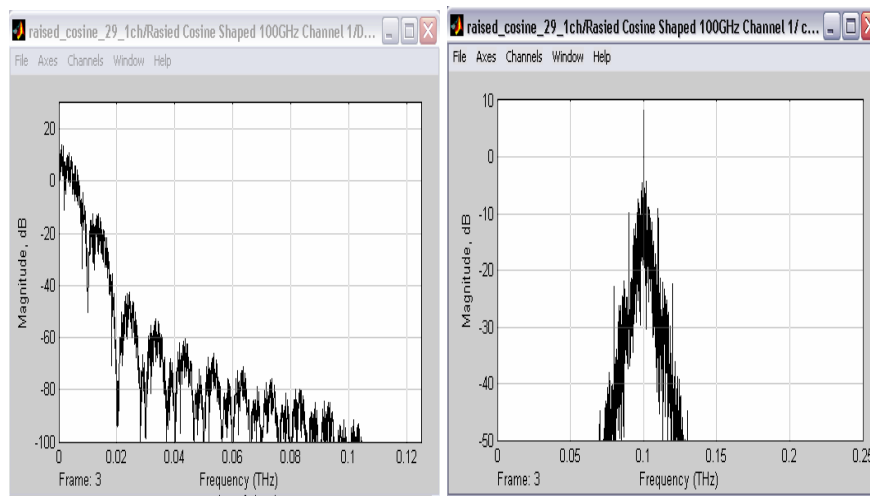
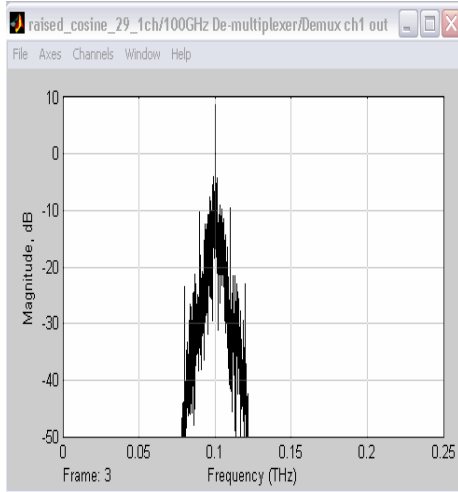


Figure 15: SIMULINK model for the modulation of raised cosine NRZ PRBS.

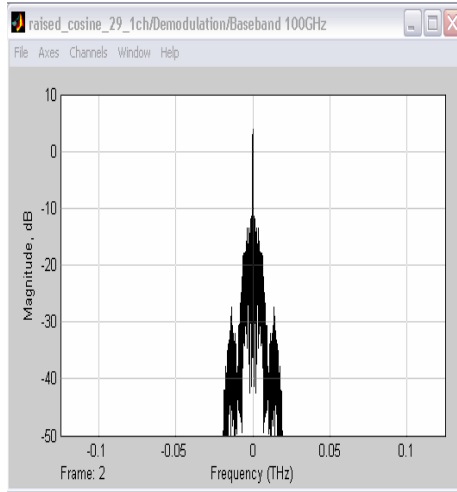


(a)

(b)

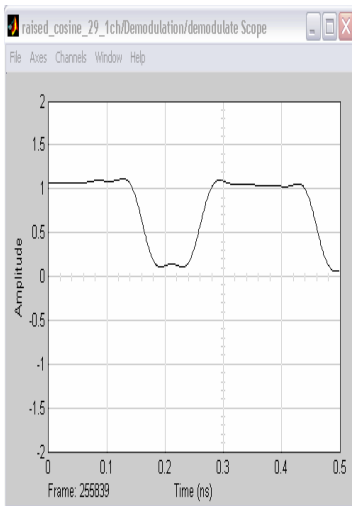


(c)

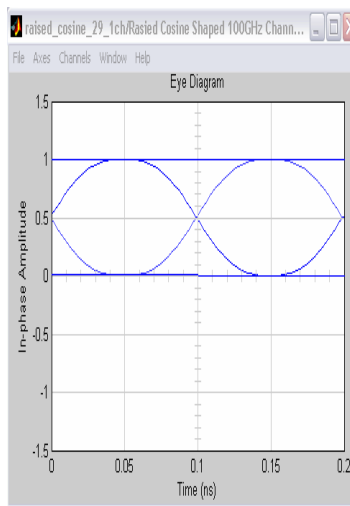


(d)

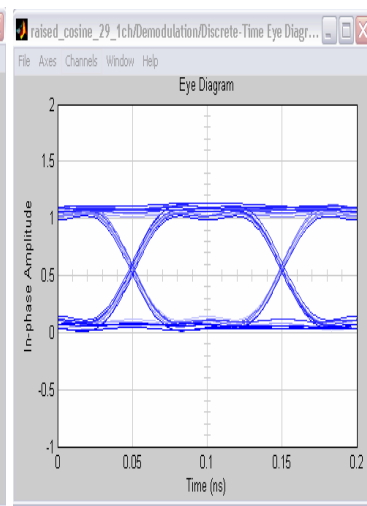
Figure 16: (a) Spectrum of raised cosine NRZ format lightwaves at base band (b) Spectrum of the raised cosine modulated lightwaves (c) Demultiplexed spectrum of the raised cosine modulation lightwave channel, back to back test (d) Spectrum of demodulated raised cosine PRBS.



(a)



(b)



(c)

Figure 17: Demodulated sequence of raised cosine pulses (b) Eye diagram of the NRZ raised cosine PRBS at the transmitter and (c) Eye Diagram of the raised cosine pulse sequence, error free at BER = 10^{-12}

4 WDM channels

Multiplexer transfers the multi laser source signals into a single mode optical fiber. “Addition” block (Figure 18) does not affect frequency spectrum of channel because each channel occupies at difference frequencies. In addition, it can add up several sources into a single frequency domain spectrum.

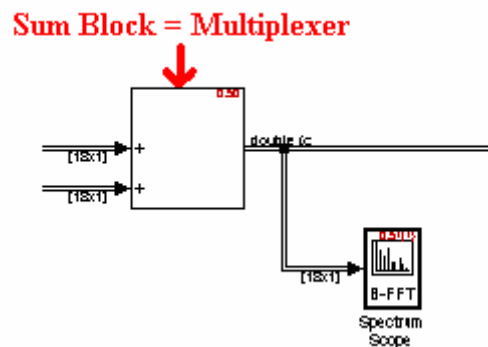


Figure 18: Multiplexer (MUX) block diagram

Before the various wavelength signals enter the receiver end, a de-multiplexer is required to separate the signals with various wavelengths. Bandpass filter as shown in Figure 19 is used to demultiplex different wavelength signals.

De-multiplexer System
The parallel Bandpass filter is used to separate each channel wavelength.

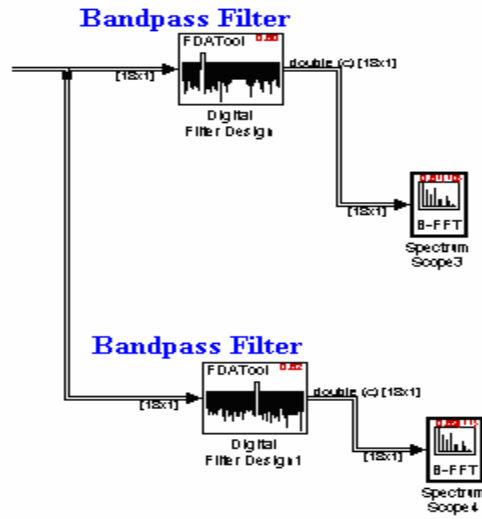


Figure 19: De-multiplexer (Demux) block diagram

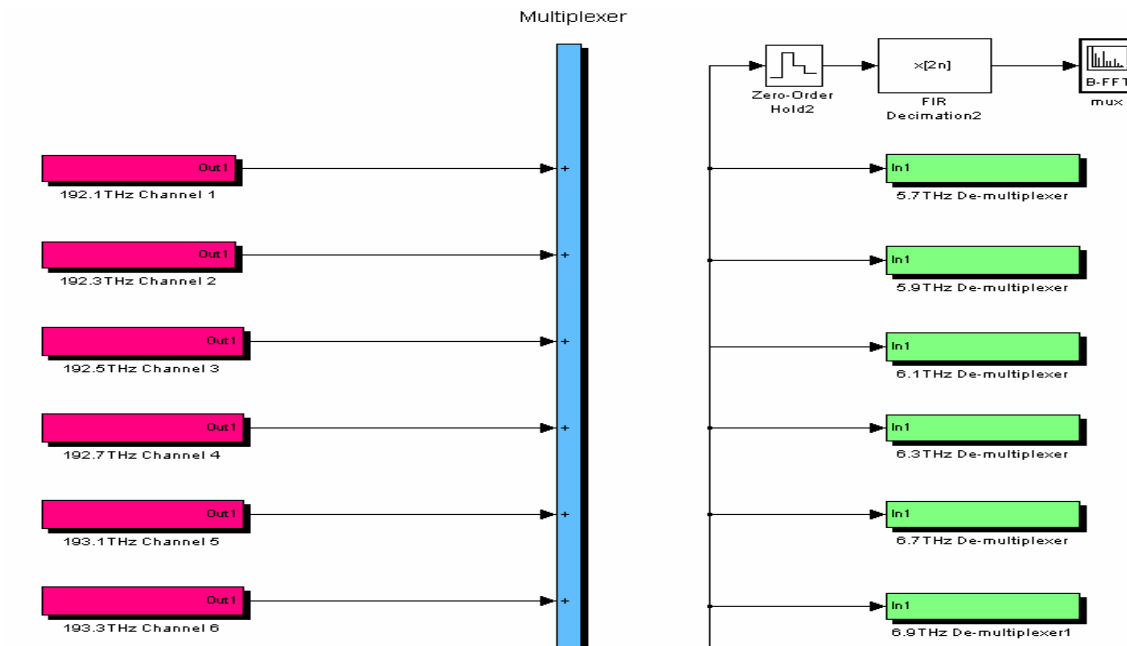


Figure 20: 16 channels Simulink Platform

Phase Modulation (PM) is a form of modulation which encodes the information into a carrier wave by variation of its phase in accordance with an input signal. The phase $\theta(t)$ of the carrier signal can be represented including the signal as

$$s(t) = A_c \cos (2\pi f_c t + \theta(t)) \quad (7)$$

The phase is proportional to the message signal $m(t)$ as

$$\theta(t) = K_c m(t) \quad (8)$$

Hence the phase modulated optical signal is then

$$S_{PM}(t) = A_c \cos (2\pi f_c t + K_c m(t)) \quad (9)$$

If the input RF signal is $m(t)$ as a function of time t , then the output is where f_c is the Carrier frequency parameter, θ is the Initial phase parameter, and K_c is the Modulation constant parameter.

The carrier frequency sets as channel carrier frequency, while the initial phase is normalized with the biased voltage at the minimum transmission point of the optical-voltage transfer characteristic curve. Inside the MZIM the incoming lightwave signal is equally split into two arms. The phase difference between two arms changes depending on the signal level and the bias voltage. Modeling of the phase difference can be implemented by a multiplication of input data signal with K_c assigned as the modulation index between the RF signal $m(t)$ and the biased voltage. Therefore, the phase modulated signal finally becomes

$$S_{PM}(t) = A_c \cos (2\pi f_c t + \pi/2 + \pi m(t)) \quad (10)$$

Figure 21 the SIMULINK block diagram of the phase modulation for one path of the MZIM.

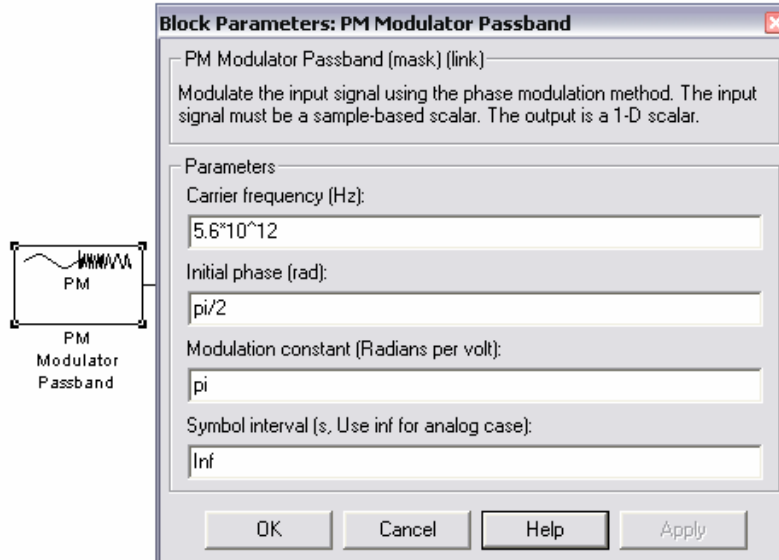


Figure 21: The Block Properties of PM modulator.

The external modulator MZIM recombine the two arms signals, if the two signals are in phase, constructive signal is formed. The two in-phase signals are added to give a maximum signal output. If the two signals are out of phase, destructive signal is achieved. Thence, the signal output is either “1” or “0”. **Figure 22** illustrates the Simulink block diagram of the modulation principles of the MZIM. If Gaussian pulse stream is required then the Simulink blocks of **Figure 23** can be used. **Figure 24** thus illustrate an exemplar of the signals at the end of a modulated path and the MZIM output.

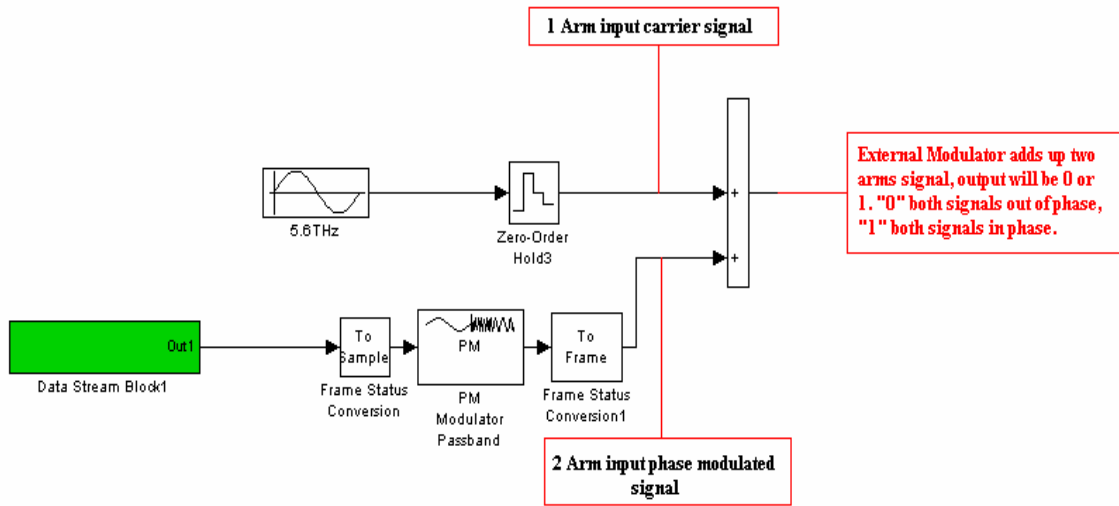


Figure 22 Block diagram of the external MZIM

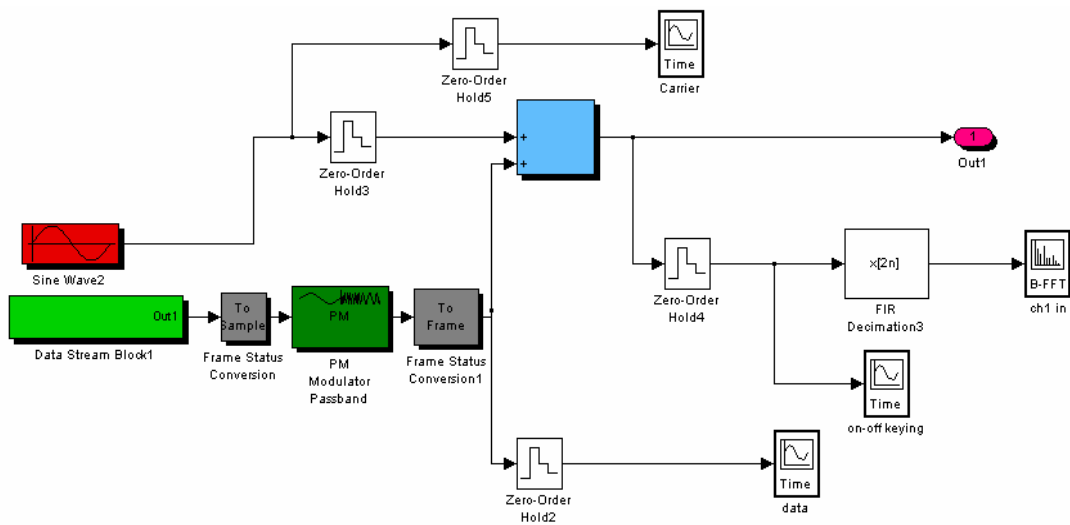


Figure 23 Gaussian shaped modulating channel input of the Simulator.

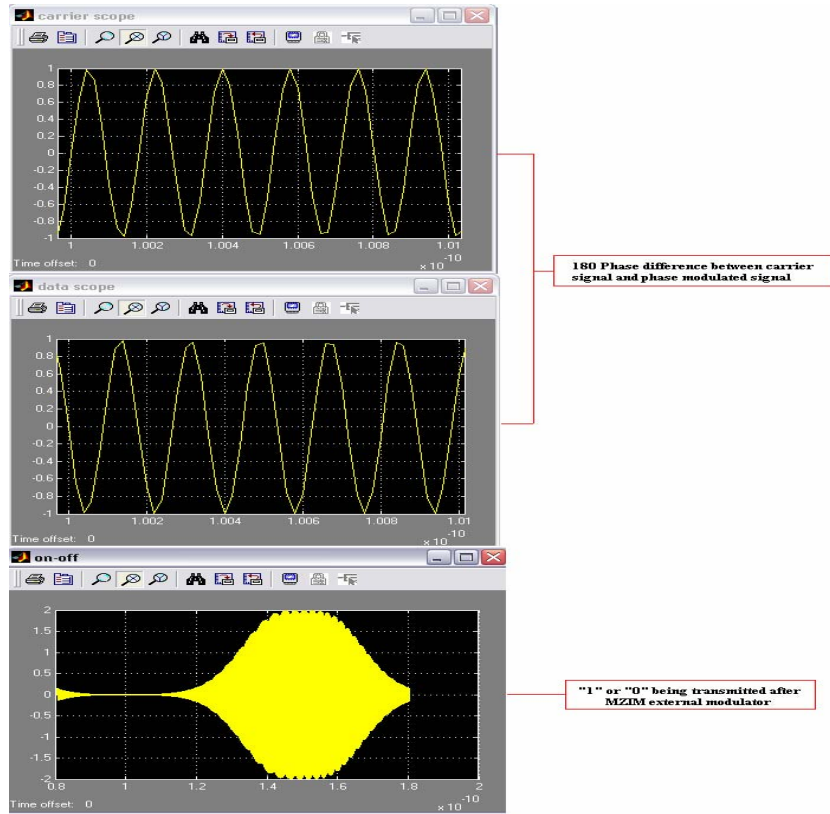
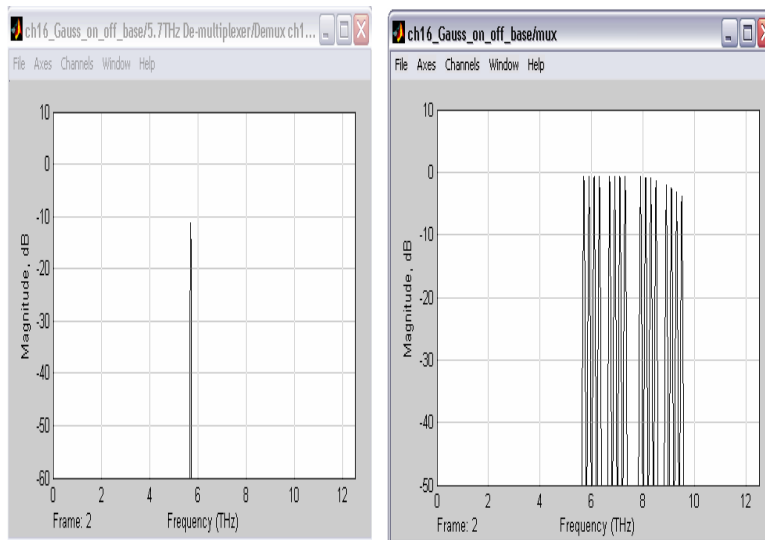


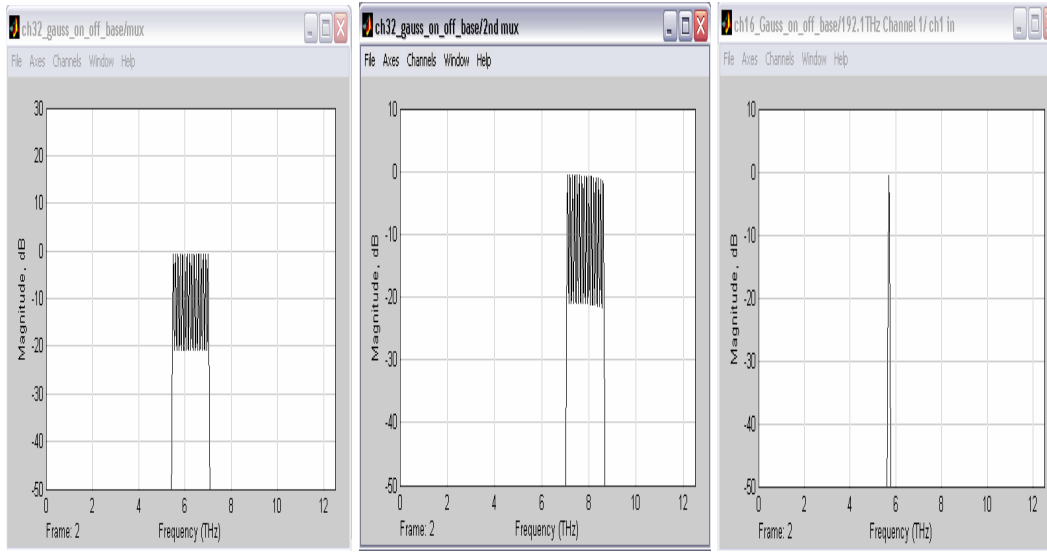
Figure 24 Carrier frequency, phase modulated signal and MZIM output time-dependent signal.



(a)

(b)

Figure 25 Spectrum of (a) a Gaussian-shaped data stream at 192.1THz (5.7THz represents) Input signal with 200GHz and (b) 16 multiplexed channels of 200 GHz channel spacing.



(a)

(b)

(c)

Figure 26 (a) The first 16 channels spectrum signal in 32 channels platform (b)The second 16 multiplexed channels and (c) Spectrum of a de-multiplexed channel 1 192.1THz (5.7THz is the scaled down centre frequency) in passband.

4.1 RZ- format demodulation

Demodulation is a technique which demodulates the modulating signal from the modulated carrier signal. The demodulation can be expressed as follows:

The modulated signal is represented as:

$$u(t) = A_c \cos(2\pi f_c t) * m(t) \quad (11)$$

The demodulated signal is:

$$s(t) = A_c \cos 2\pi f_c t * u(t) = \frac{A_c^2}{2} [\cos 4\pi f_c t + 1] m(t) \quad (12)$$

Therefore, the low pass filter (LPF) is used to filter the high frequency components of the signal, hence demultiplexing the channel (10 Gb/s Gaussian shaped signal) after the demodulation Simulink sub-system as shown in *Figure 27*.

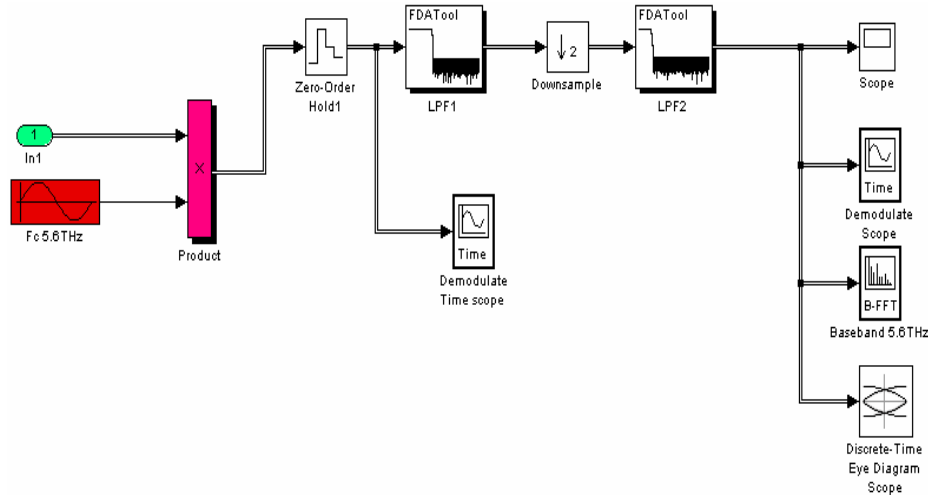


Figure 27: Demodulation Simulink Platform

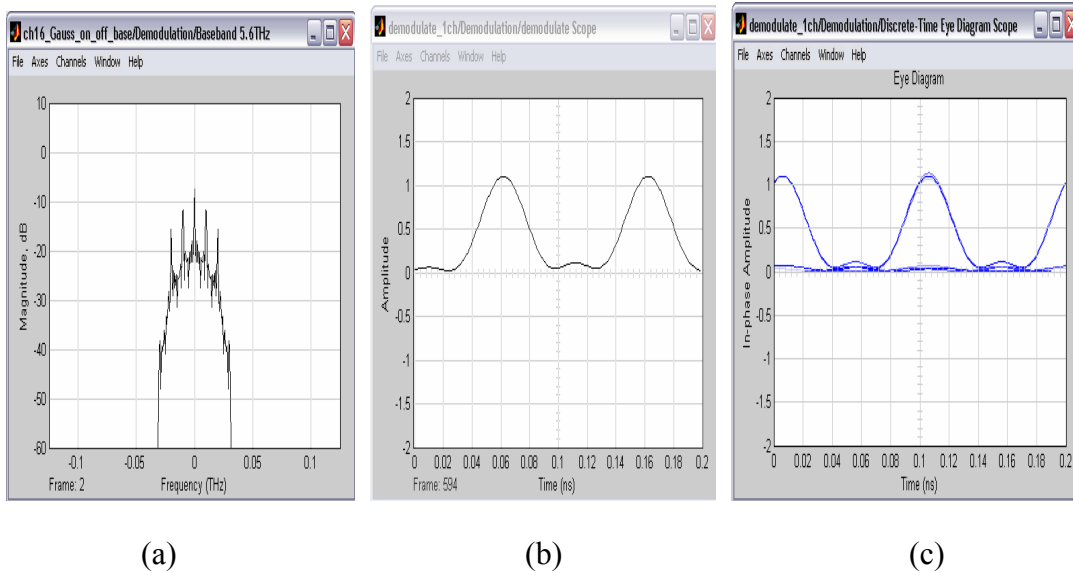


Figure 28 (a) Spectrum of the de-modulated RZ-ASK data stream (b) de-modulated output signal (10Gb/s Gaussian shaped) (c) Eye diagram of the de-modulated output signal (10Gbps Gaussian shaped) - $Q= 7$, BER 10^{-12}

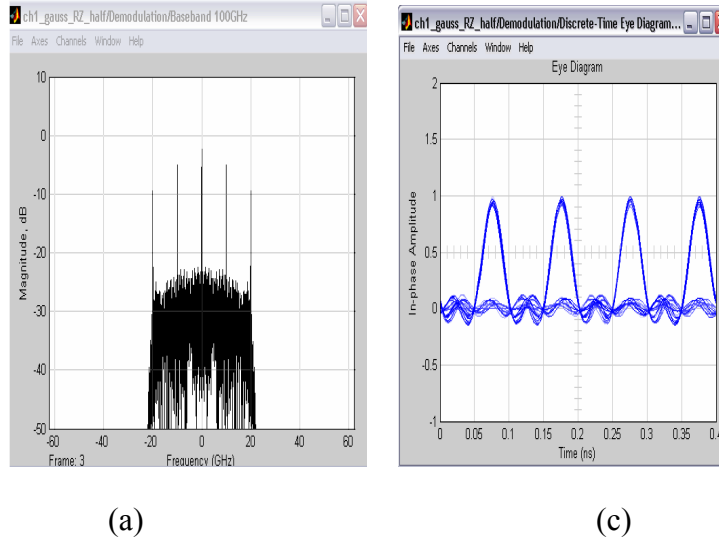


Figure 29: (a) RZ Gaussian pulse shaped demodulated signal spectrum using high resolution sampling (b) RZ Gaussian pulse shaped eye diagram signal at the output of the demodulator.

5 Dual electrode MZ Modulator: Simulation and Experimental Results

5.1 Dual electrode MZ Modulator DSB Simulation

The output field of the dual driven MZIM can be represented as[6]

$$E(t) = A/2\{ \cos(\omega_c t + \gamma\pi + \alpha\pi \cos\omega_{rf}t) + \cos(\omega_c t + \alpha\pi \cos\omega_{rf}t + \theta) \} \quad (13)$$

where ω_c is the optical carrier frequency ; $\gamma\pi$ is the bias factor of each arm of the MZIM, $\alpha\pi$ - optical modulation index. ω_{rf} is the RF frequency of the signal. From the transfer characteristic curve of experiment that we can find that $\gamma\pi = \pi V_{dc}/V_\pi = 1/2\pi$, and $\alpha\pi = \pi V_{ac}/V_\pi = 1/3 \pi$ with $\theta = \pi$ with V_π is the minimum transmission voltage of the MZIM, V_{ac} is the amplitude of the input drive signal. The Simulink sub-system for the dual drive MZIM is given in **Figure 30**. The frequency spectrum of the dual drive modulator is given in **Figure 31**.

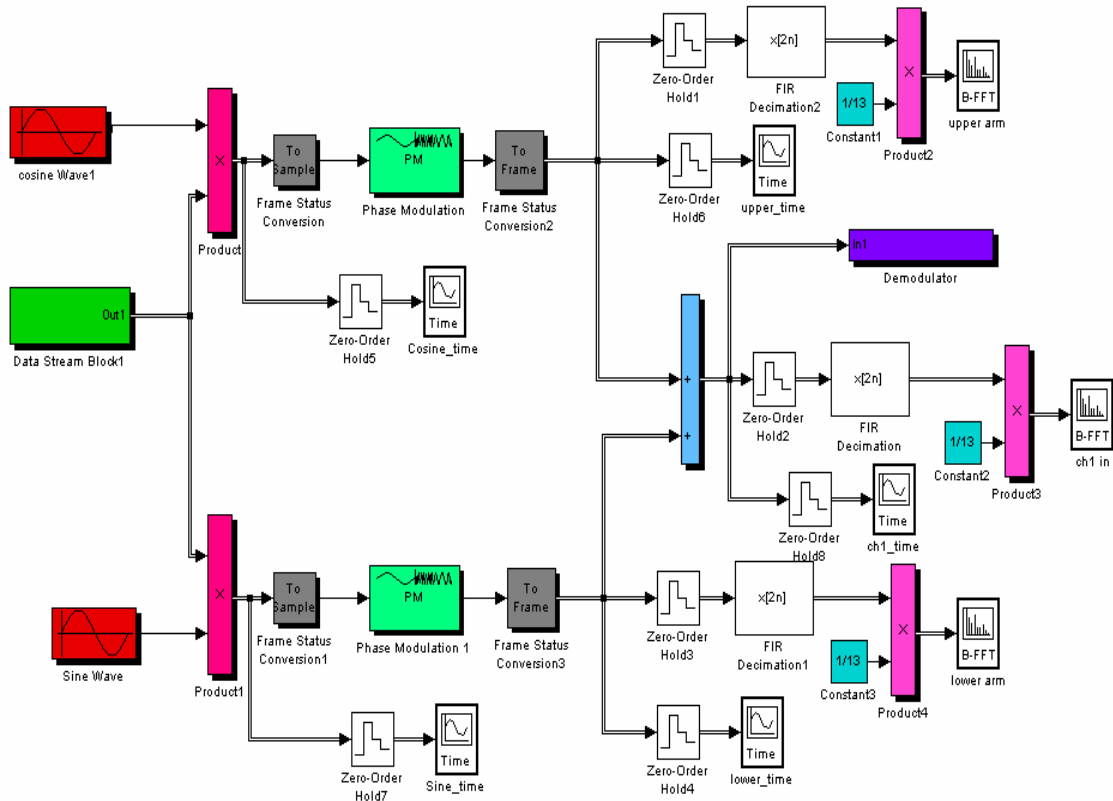
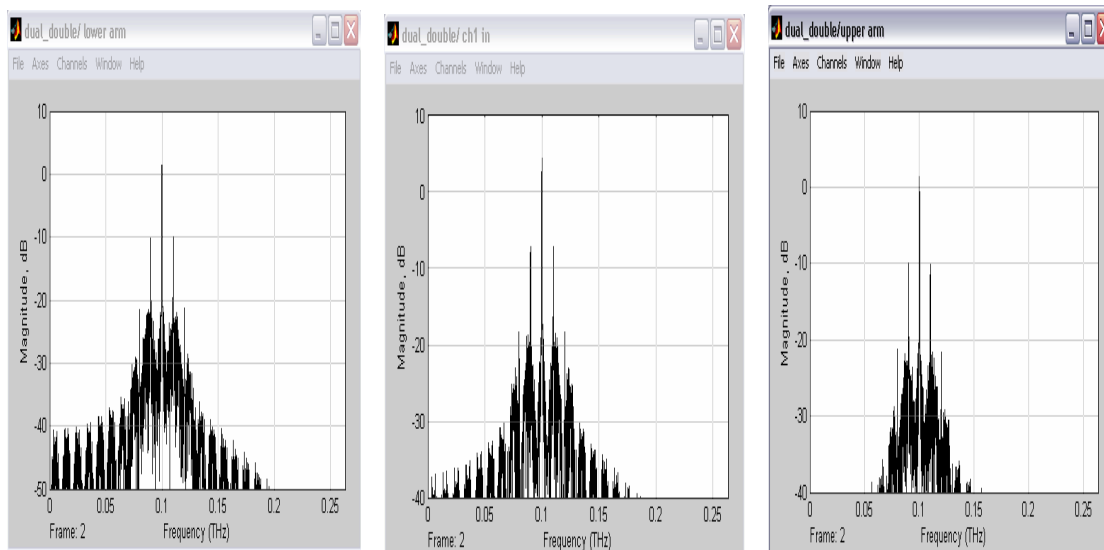


Figure 30: Dual electrode MZ DSB Modulator



(a) (b) (c)

Figure 31: (a) Upper Arm of Dual electrode MZ modulator $\cos(\omega_c t + \gamma\pi + \alpha\pi \cos\omega_{rf}t)$ (b) Lower Arm of Dual electrode MZ modulator $\cos(\omega_c t + \alpha\pi \cos\omega_{rf}t + \theta)$ and (c) Dual Electrode MZ modulator DSB output spectrum.

5.2 DSB Carrier Suppressed (DSB-CS) modulation using dual drive MZIM

Similar to the case of RZ ASK modulation, the carrier suppress DSB (CS-DSB) requires lower optical power that decreases nonlinear effects. Furthermore due to the suppression of the high power carrier signal, optical amplifiers can be placed immediately after modulator to boost the signals to a maximum level. Mathematically we can express[6]

$$E(t) = A/2\{ \cos(\omega_c t + \gamma_1\pi + \alpha\pi \cos\omega_{rf}t) + \cos(\omega_c t + \gamma_2\pi + \alpha\pi \cos\omega_{rf}t + \theta) \} \quad (14)$$

where ω_c - carrier radial frequency, $\gamma\pi$ - bias of each of the arm, $\alpha\pi$ - optical modulation index and ω_{rf} is the radial frequency of the RF signal. From the characteristic curve of experiment that we can find that $\gamma_1\pi = \pi V_{dc}/V_\pi = 1/2\pi$, $\gamma_2\pi = \pi V_{dc}/V_\pi = -1/2\pi$, $\alpha\pi = \pi V_{ac}/V_\pi = 1/3 \pi$ and $\theta = \pi$. Figure 32 shows the Simulink block diagram of the modulation scheme.

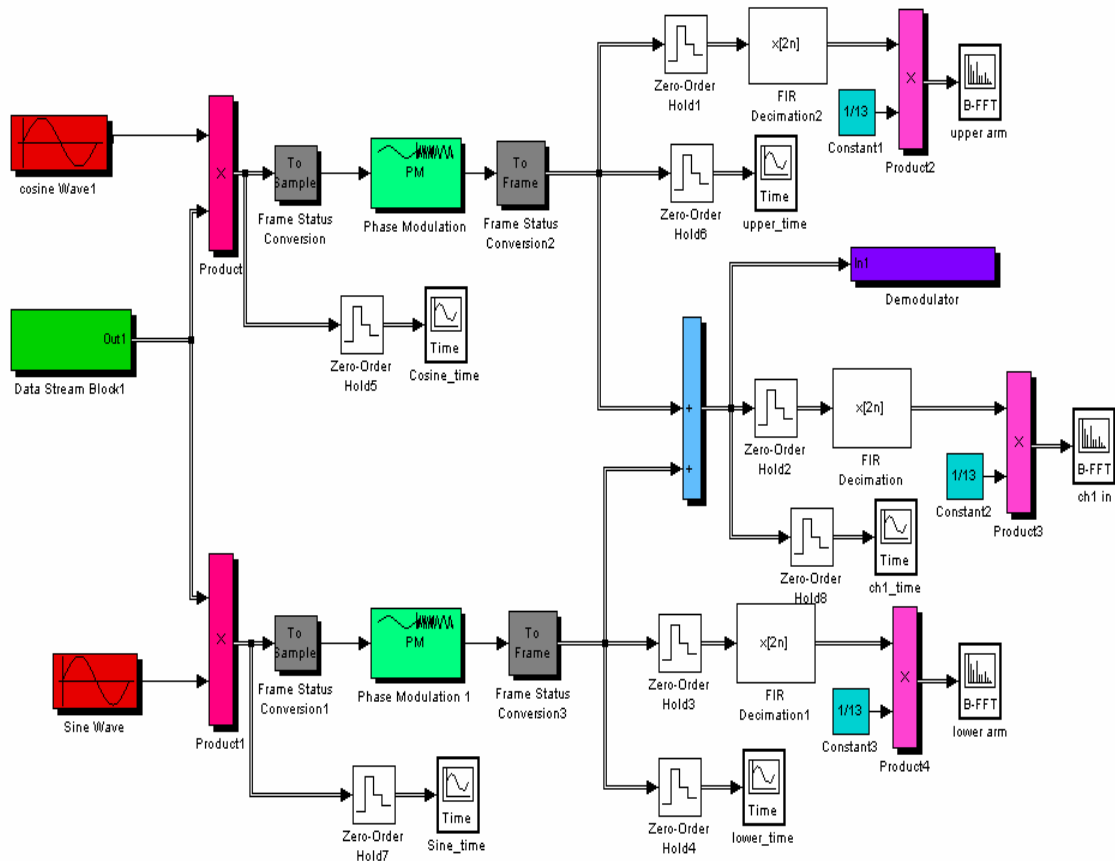


Figure 32 Simulink model of the dual-drive DSB MZIM

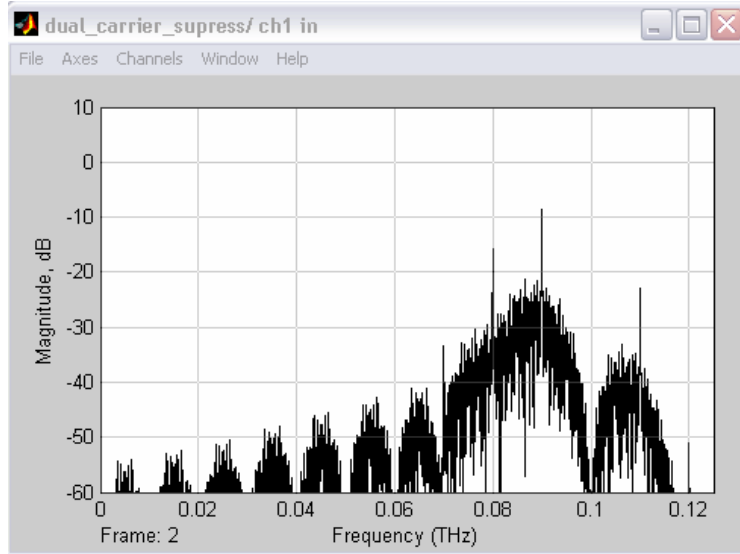


Figure 33 Dual Electrode MZ modulator DSB CS spectrum result

5.3 SSB Simulation

Again the modulation of the optical paths of the MZIM can be mathematically represented as[7]:

$$\text{Output of the modulator arm 1} = \sin \omega_c t * \sin \omega_m t = \frac{1}{2} \cos(\omega_c - \omega_m)t - \frac{1}{2} \cos(\omega_c + \omega_m)t \quad (15)$$

$$\text{Output of the modulator arm 2} = \cos \omega_c t * \cos \omega_m t = \frac{1}{2} \cos(\omega_c - \omega_m)t + \frac{1}{2} \cos(\omega_c + \omega_m)t \quad (16)$$

$$\begin{aligned} & \frac{1}{2} \cos(\omega_c - \omega_m)t - \frac{1}{2} \cos(\omega_c + \omega_m)t \\ \text{Therefore, the output signal} & = \frac{+ \frac{1}{2} \cos(\omega_c - \omega_m)t + \frac{1}{2} \cos(\omega_c + \omega_m)t}{\cos(\omega_c - \omega_m)t(LSB) \& \text{cancel}(USB)} \quad (17) \end{aligned}$$

Figure 34 shows the block diagram of the Simulink simulator of SSB modulation scheme. The monitor of the modulated lightwaves propagating in the two arms are given in **Figure 35**. Their corresponding spectra shown in **Figure 36** (a), (b) and (c) indicate clearly the upper, lower sideband and the composite SSB respectively. Note no display of the phases are possible due the nature of the 1-D Fourier transform.

SingleSide Band Modulation System

Student: Yuk Lan Cheung (18099300)
 Supervisor: Dr. L. N. Binh

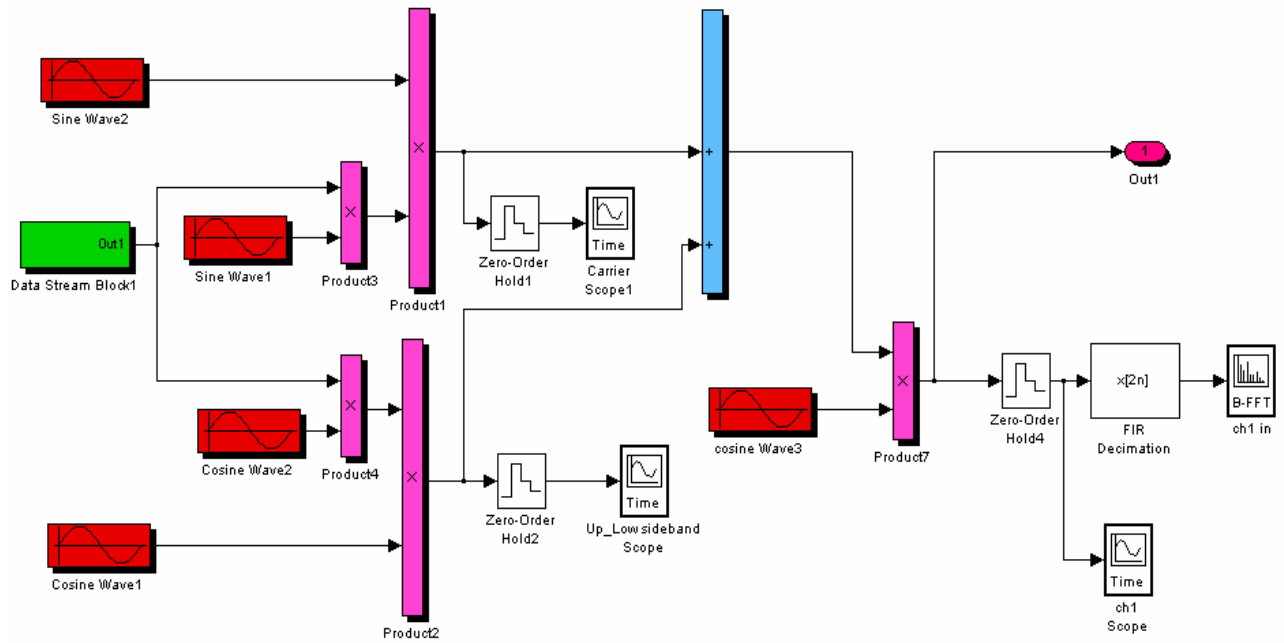
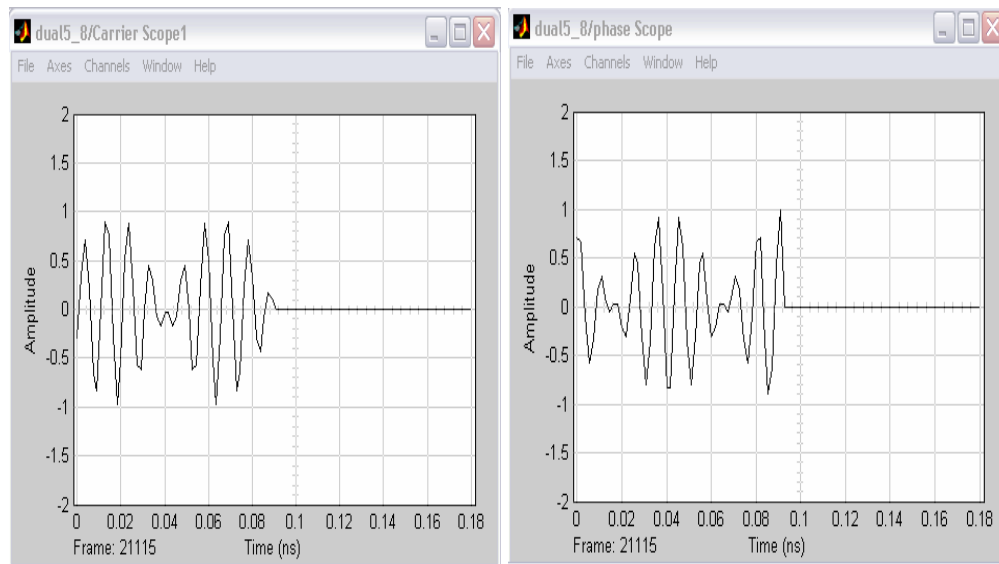


Figure 34 Simulink sub-System for Single Side band Modulation



(a)

(b)

Figure 35 (a) Upper modulation arm signals: $\sin\omega_{mt} * \sin \omega_c t$ (b) Lower Modulation arm signals: $\cos\omega_{mt} * \cos \omega_c t$

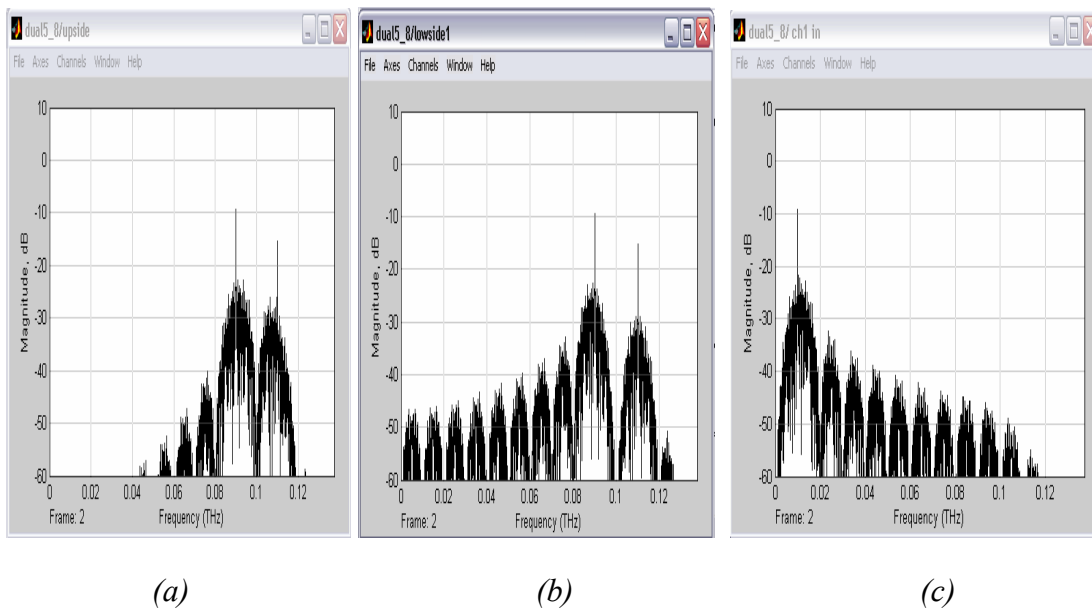


Figure 36 (a) Upper and lower sideband spectrum at the upper arm (b) Upper and lower sideband spectrum at the lower arm and (c) SSB signal spectrum without Carrier.

5.4 Modulation formats Experiments: Single, Cascade and Dual electrode MZIM

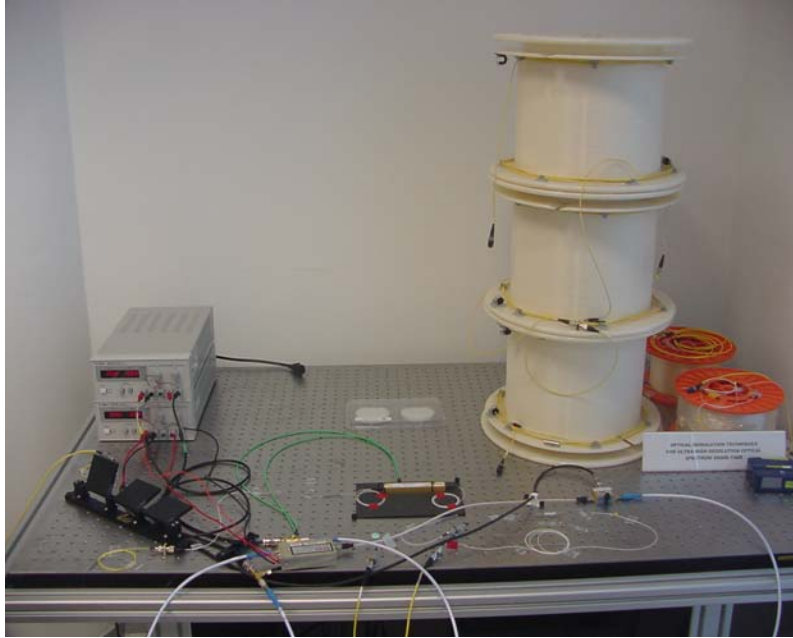


Figure 37 Dual-Drive MZIM Experiment Set-up.

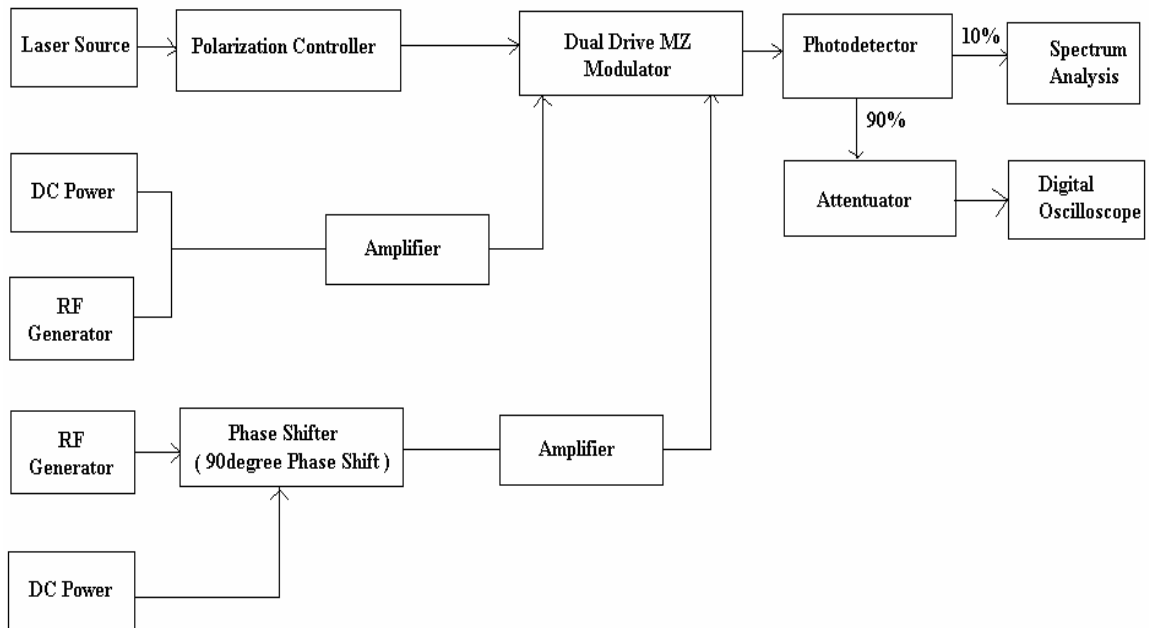
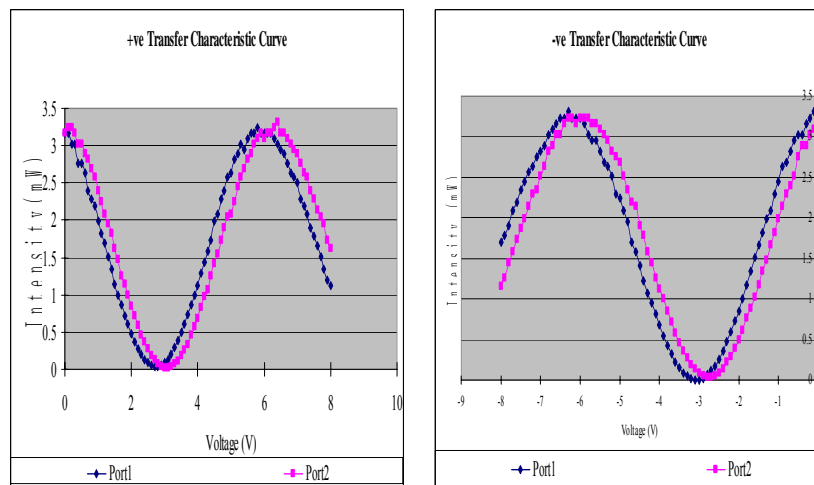


Figure 38: Schematic Diagram of the Dual-Drive MZ Modulator Experiment Set-Up.

In Figure 38 shows the Dual drive MZ modulator diagram model. The laser is 1550.44nm going into the polarization controller to minimize the polarization effects to get the maximum power signal. Furthermore one of RF signals is amplified and the other is $\pi/2$ phase shifted (SSB) or π (DSB) and the amplified go into the dual drive MZ modulator. There are two bias voltages controlling the dual-drive MZ modulator. The bias voltages are determined from the transfer characteristic curves in Figure 39. At the receiver end, the photodetector is used to detect and transfer the optical signal into electrical signal and through using the 90:10 couplers to show in the oscilloscope and spectrum scope. If any signal higher than 5dB has to use attenuator else the photodetector would be damaged.



(a)

(b)

Figure 39: (a) Positive (b) negative Transfer Characteristic Curve of Dual Drive MZIM dual-bias.

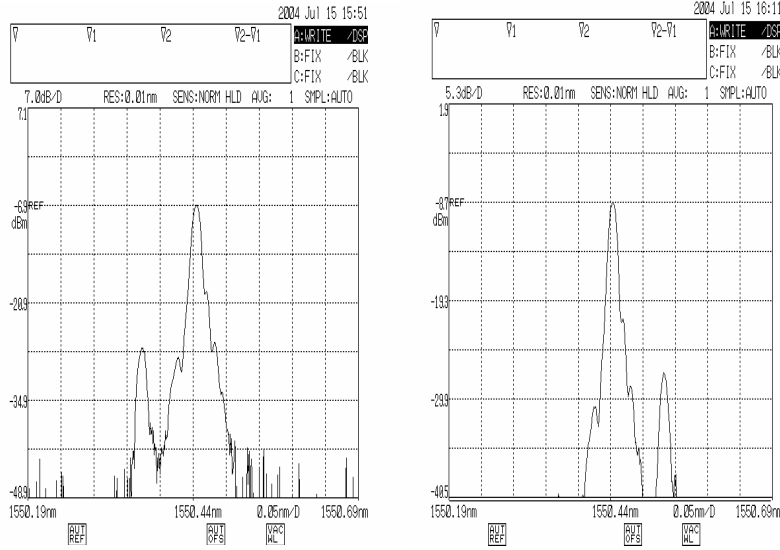


Figure 40 Output of the dual-drive MZ SSB modulator at 1550.44nm with (a) lower SSB
(b) Upper SSB

	Lower Sideband	Upper Sideband
Input Laser Source	10dBm	10dBm
Wavelength	1550.44nm	1550.44nm
Input Data Rate	10GHz at 18dBm	10GHz at 18dBm
Port1 controller	4.15V	4.15V
Port2 controller	5.13V	5.13V
Phase Shifter controller	8.4V	8.4V
Amplifier Bias Voltage Controller	2.9V	2.9V
Output with no fiber	3.5dBm	3.5dBm

Table 1 Dual Drive MZIM SSB experimentally measured parameters

Dual drive MZ Modulator has high loss where its fiber connectors and splice attribute some loss, polarization about 1dB. The refractive index (LiNbO_3) of that arm (or both arms in dual electrode MZIM) is changed due to the electro-optic effect in the medium by applying a voltage to the electrode.

The modulator significant losses are incurred when coupling the laser from fiber to the channel waveguide. Therefore, a marginal 5 dB loss in modulator is acceptable. Laser entering the modulator has fix polarization. The polarization exists of the two arms are asymmetrical. In theoretical, the fiber loss is 0.2dB/km. In the experiment, after connecting 20km fiber which suppose has 4dBm loss. The output signal power in the

receiver is 0.5dBm, so that the fiber loss in the experiment is 3dBm after the signal transmitted through 20 km SSMF.

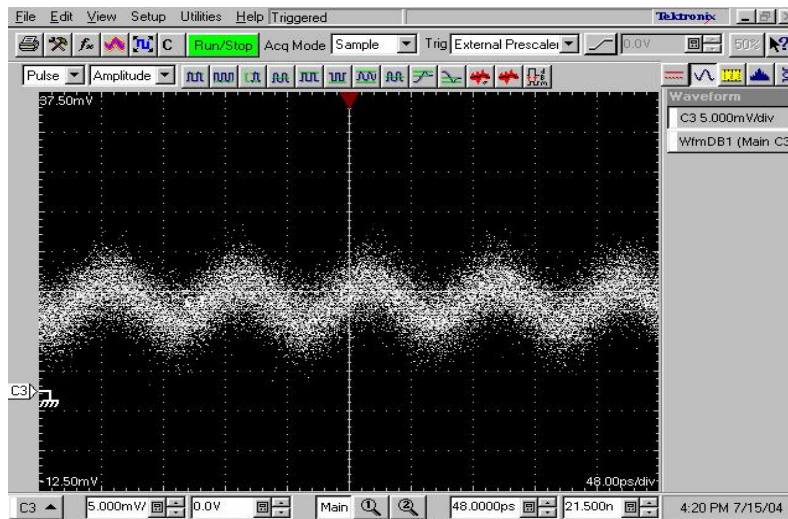


Figure 41 Dual Drive MZ SSB Modulator Output Signal Power of 0.5dBm, without optical preamp..

Experimental set-up for modulation at 40 Gb/s is shown in **Figure 42** . A $2^{31}-1$ PRBS pattern generator is used to drive the MZIM transmitter (SHF 5008). The output of the Tx is boosted to appropriate optical power level and then sent through an optical Mux then optically amplified and then demuxed and detected via the Rx SHF 5003. The received eye diagram is then displayed in a sampling oscilloscope. The bit-error-rate is then counted with an error analyzer SHF- EA 4. **Figure 43** shows the optical spectra of the modulated PRBS sequence. The spectra confirm the side bands and the carrier suppressed RZ and NRZ. **Figure 44** shows the variation of the BER as a function of the received optical power (not including the 10 dB of the attenuator).

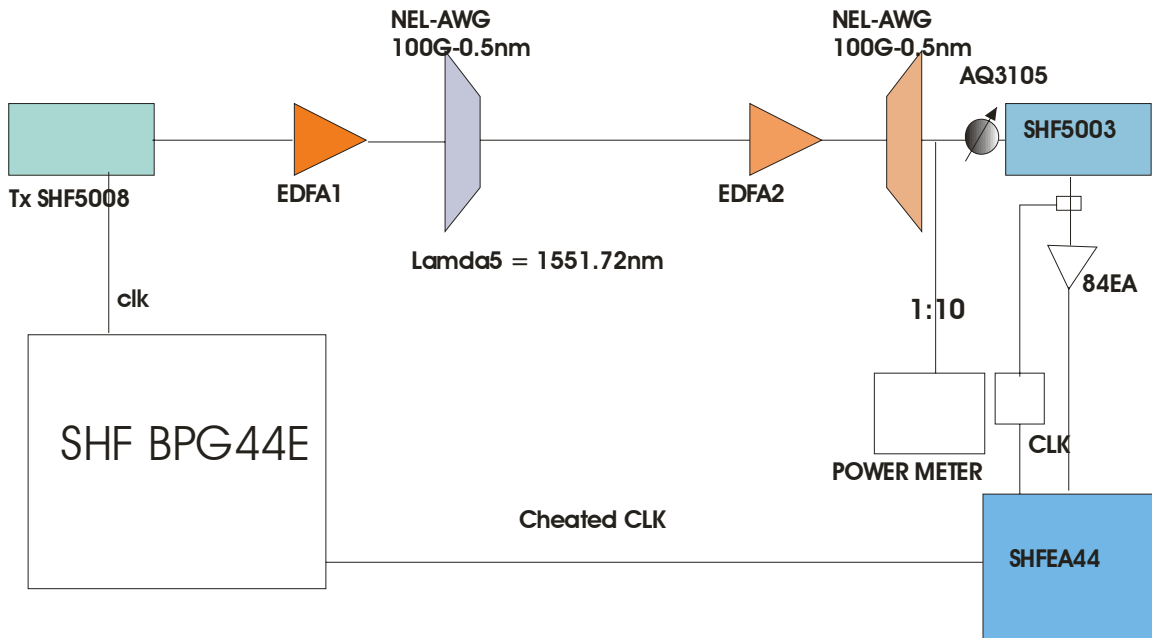


Figure 42 40 b/s optical modulation system set-up back to back with optical filters, optical amplifiers and MUXES and DEMUXES.

Spectral Responses from Various Modulation Formats

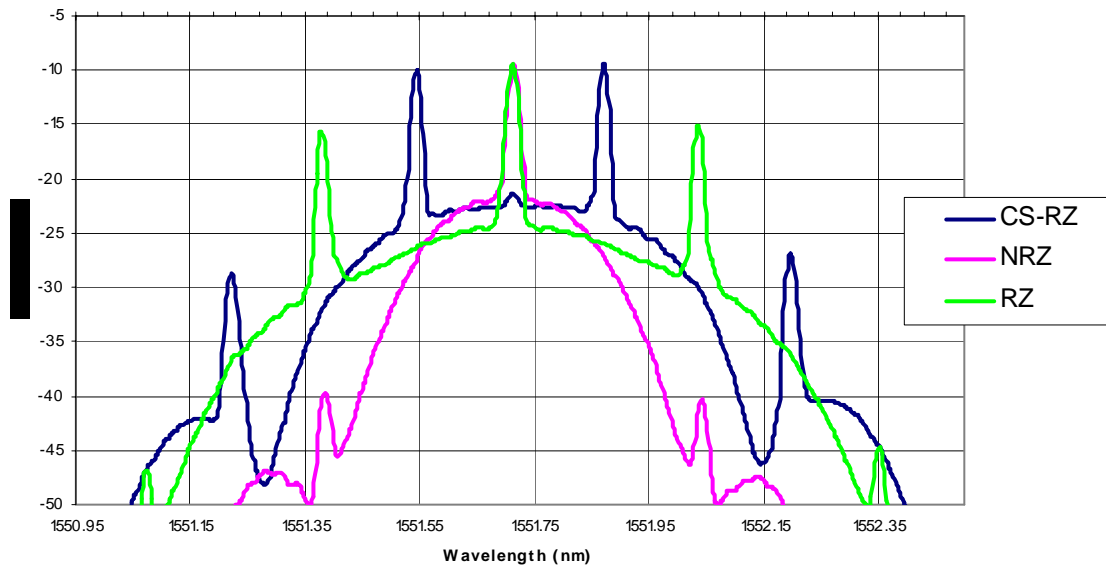


Figure 43 Optical spectra CS-RZ, NRZ and RZ at 40 Gb/s

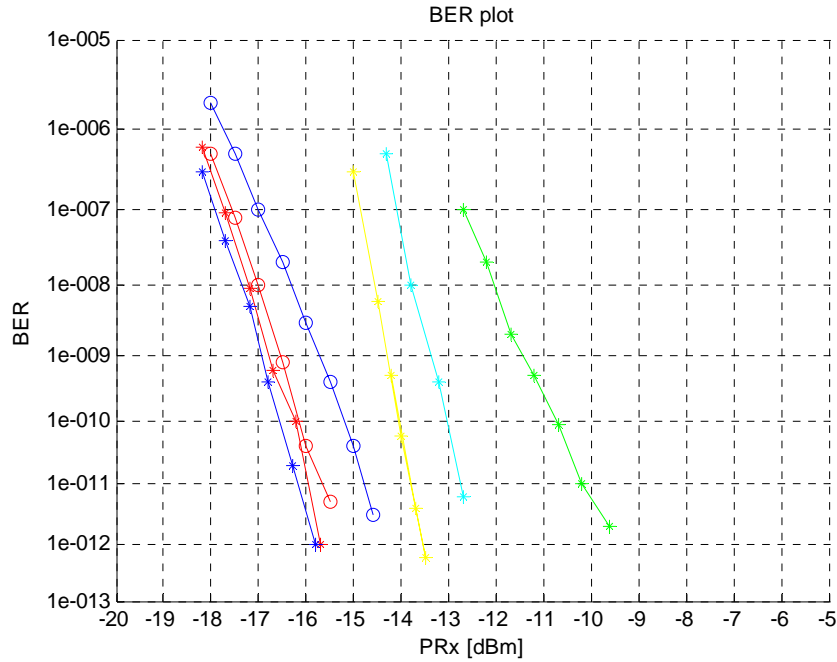


Figure 44 BER versus received optical power (at the power meter – 1;10 coupler before Rx). Legends: “blue” CSMZ-DPSK (one NELAWG); “red” – RZ DPSK(one NELAWG); “green” NRZ ASK(one NELAWG); “yellow” – CSMZ- ASK (one NELAWG); “c” RZ-ASK(one NELAWG); Note: only one optical filter NEL AWG is used; “Red o” CSMZ DPSK TWO AWGs used; “blue o” RZ-DPSK TWO AWGs used. Note: the DPSK formats will be reported in a future document.

5.5 Dual electrode MZ Modulator SSB Simulation

The analytical expression of a dual-driven MZIM with RF signals is given by [6]

$$E(t) = A/2 \{ \cos(\omega_c t + \gamma_1 \pi + \alpha \pi \cos(\omega_{rf} t + \theta_1)) + \cos(\omega_c t + \gamma_2 \pi + \alpha \pi \cos(\omega_{rf} t + \theta_2)) \} \quad (18)$$

where ω_c - carrier radial frequency, $\gamma \pi$ - bias of each of the arm, $\alpha \pi$ - optical modulation index and ω_{rf} - RF signal. From the characteristic curve of the optical – RF voltage transfer characteristic obtained experimentally, we can find that $\gamma \pi = \pi V_{dc}/V_\pi = 15/4\pi$, $\alpha \pi = \pi V_{ac}/V_\pi = 1/3 \pi$ and $\theta_1 = 2\pi/3$ and $\theta_2 = \pi/6$ with V_π - the switching voltage of the MZ modulator and V_{ac} - the amplitude of the input drive signal.

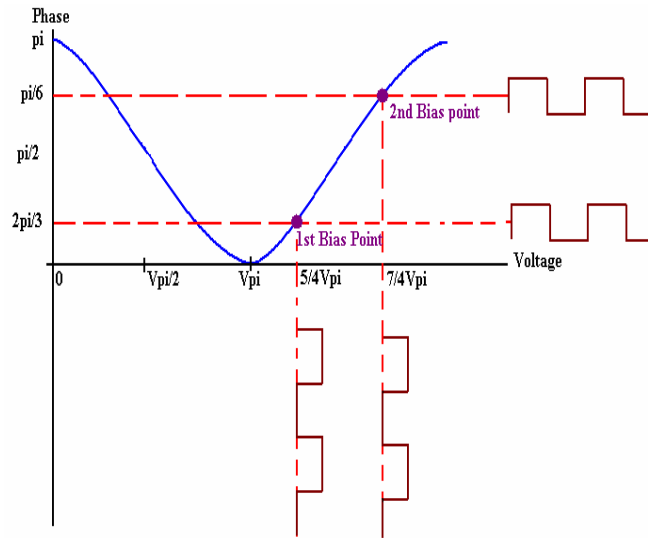


Figure 45: Phase characteristic curve to determine bias points of two arms in dual drive MZ modulator

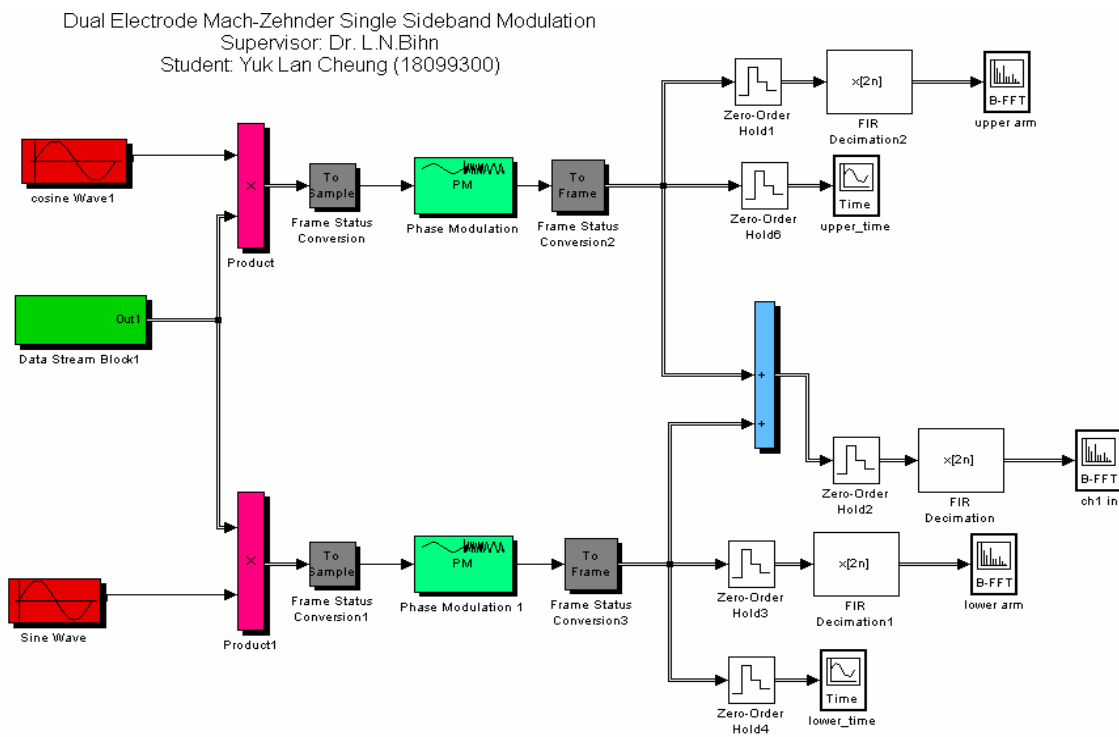
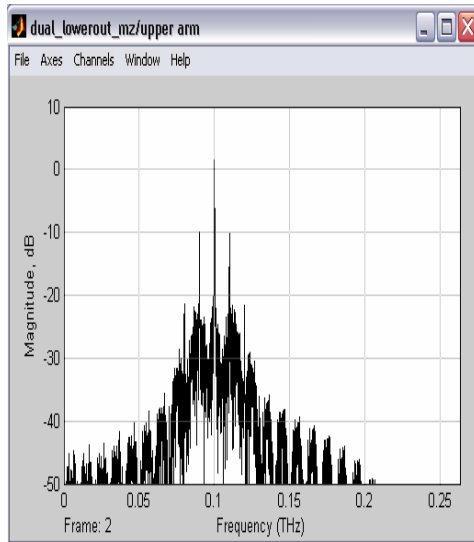
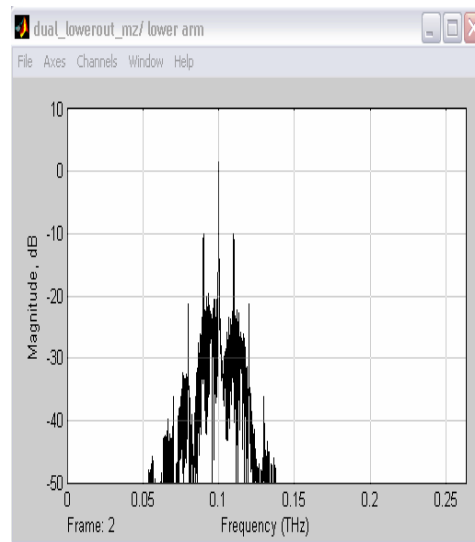


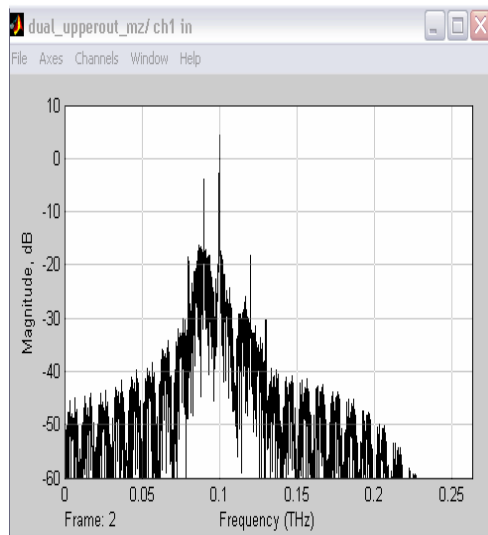
Figure 46: Dual Drive SSB MZ modulator platform



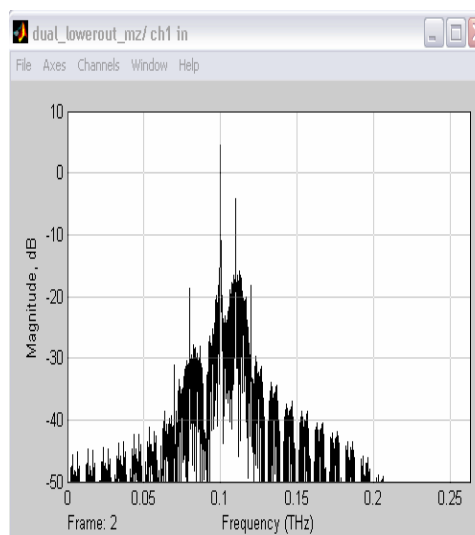
(a)



(b)



(c)



(d)

Figure 47: (a) Upper Arm of Dual electrode MZ modulator $\cos(\omega_c t + \gamma_1 \pi + \alpha \pi \cos(\omega_r t + \theta_1))$ and (b) Lower Arm of Dual electrode MZ modulator $\cos(\omega_c t + \gamma_2 \pi + \alpha \pi \cos(\omega_r t + \theta_2))$ and (c) Dual Electrode MZ modulator SSB system spectrum result with the cancellation of the upper SB (d) resultant spectrum with lower SB cancelled out

5.6 Hilbert Transform SSB MZ Modulator Simulation

The Hilbert transform of signal $m(t)$ is defined as the RF signal whose frequency components are all phase shifted by $\pi/2$ radians[7]. Thence we have

$$\hat{m}(t) = H \{m(t)\}; m(t) = A \cos 2\pi f_o t \text{ and hence } \hat{m}(t) = A \cos(2\pi f_o t - \frac{\pi}{2}) \quad (19)$$

The Fourier transform is then given by

$$M(f) = -j \operatorname{sgn}(f) \frac{A}{2} [\delta(f + f_o) + \delta(f - f_o)] = \frac{A}{j2} [-\delta(f + f_o) + \delta(f - f_o)] \quad (20)$$

Thus,
$$\hat{m}(t) = A \cos(2\pi f_o t - \frac{\pi}{2}) = A \sin 2\pi f_o t. \quad (21)$$

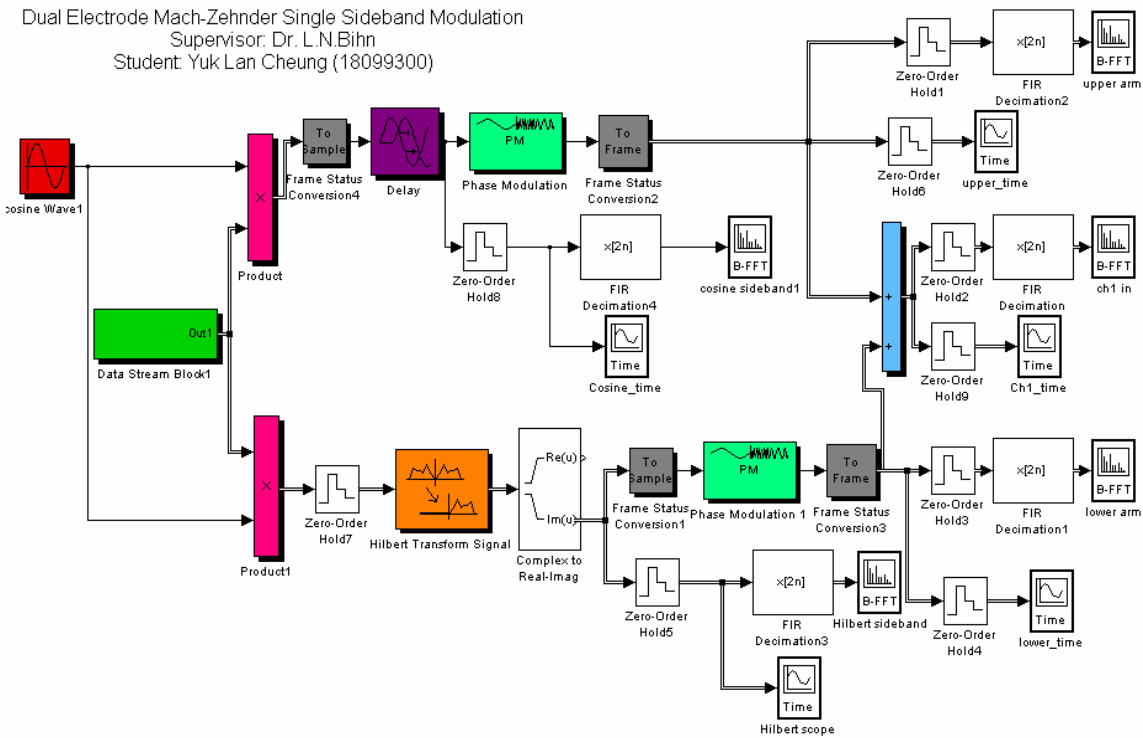
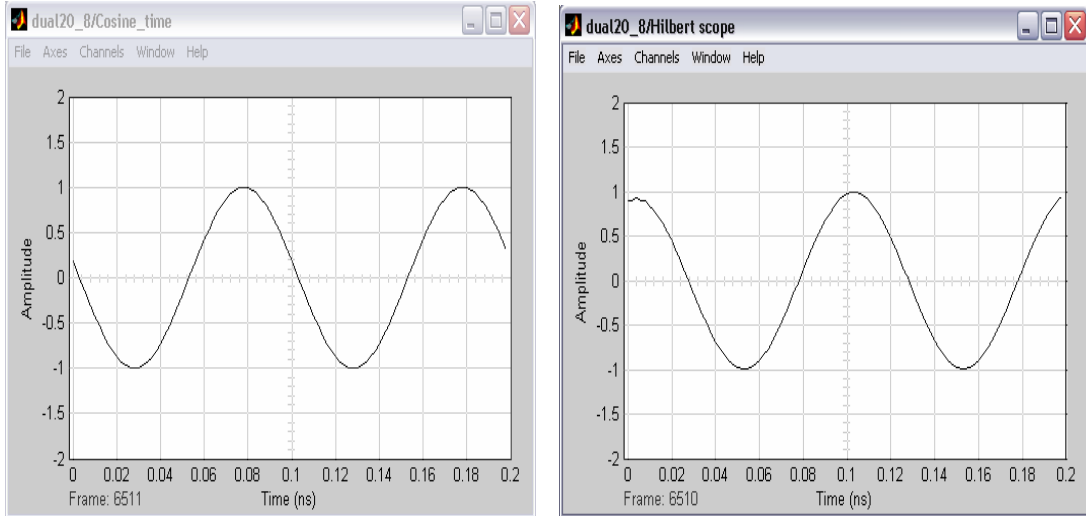


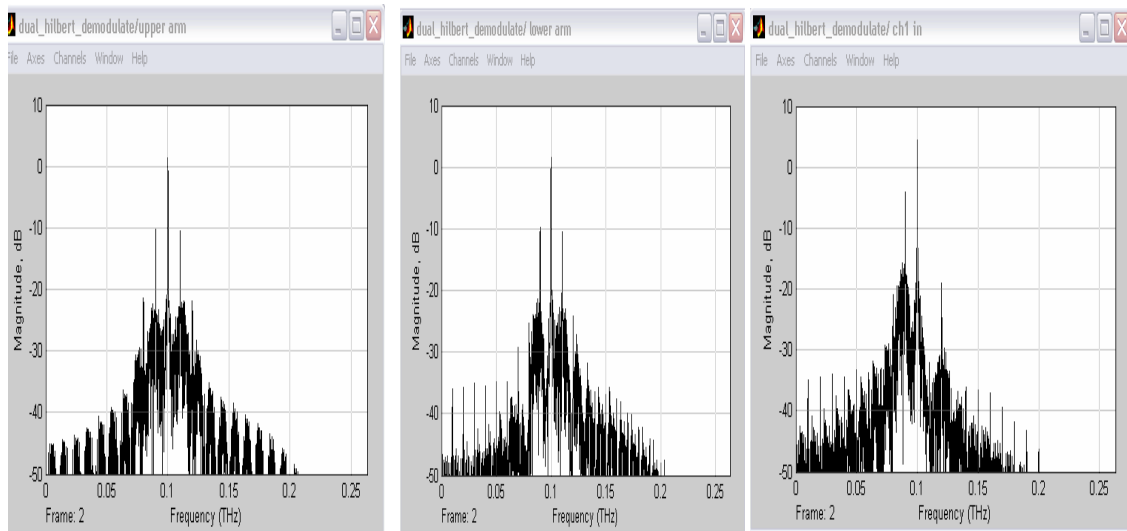
Figure 48: SSB Hilbert transform phase shifter modulator



(a)

(b)

Figure 49: (a) Input RF signal time scope (cosine signal) (b) Hilbert transform the input RF signal $H\{x(t)\} = A \cos(2\pi f_0 t - \pi/2) = A \sin(2\pi f_0 t)$



(a)

(b)

(c)

Figure 50: Upper arm of dual electrode MZ modulator with delay 10ns in Hilbert transform phase shift system (b) Lower arm of dual electrode MZ modulator with Hilbert transform phase shift $\theta = \pi/2$ and (c) Dual electrode MZ modulator SSB system spectrum result with lower SB cancels out

5.7 SSB Demodulator Simulation

The modulated signal is:

$$u(t) = A_c/2 \{ \cos(\omega_c t + \gamma\pi + \alpha\pi \cos \omega_{rf} t) + \cos(\omega_c t + \alpha\pi \cos(\omega_{rf} t + \theta)) \} \quad (22)$$

The demodulated signal is:

$$s(t) = A_c \cos 2\pi f_c t * u(t) \quad (23)$$

The LPF is used to filter high frequency components in the signal. The only component left is the modulating signal (10Gb/s [binary * cosine signal]) after the demodulation.

It is required to multiply the demodulate signal by in phase cosine signal and also there is high frequency signal, so that LPF is required to filter the high frequency components in the signal.

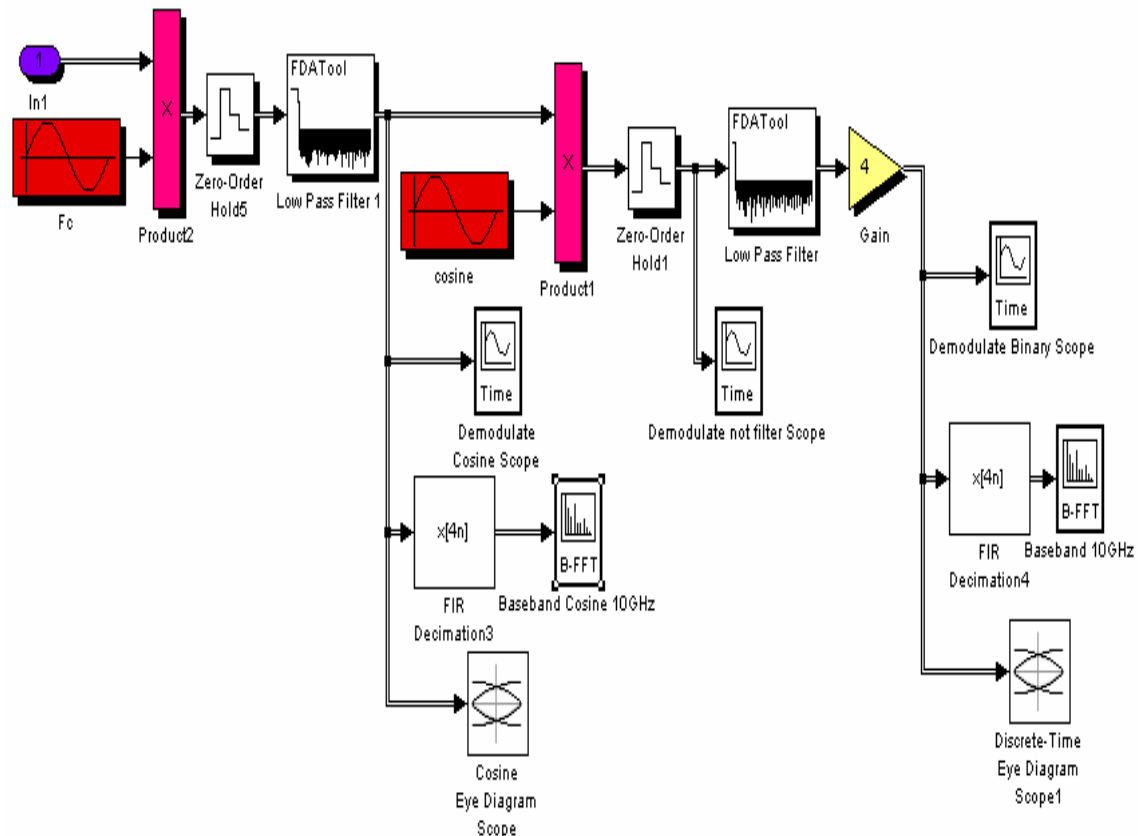
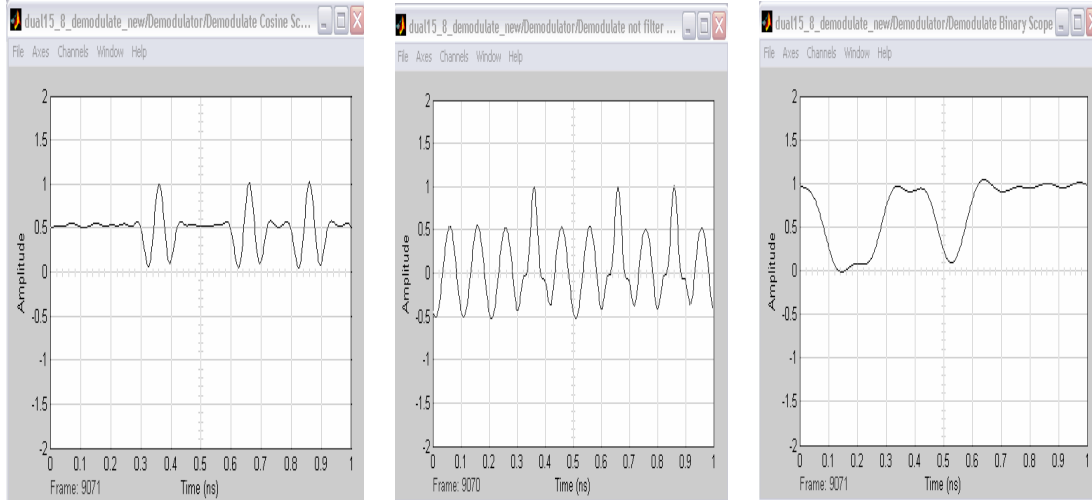


Figure 51: SSB Demodulation sub-Simulator.

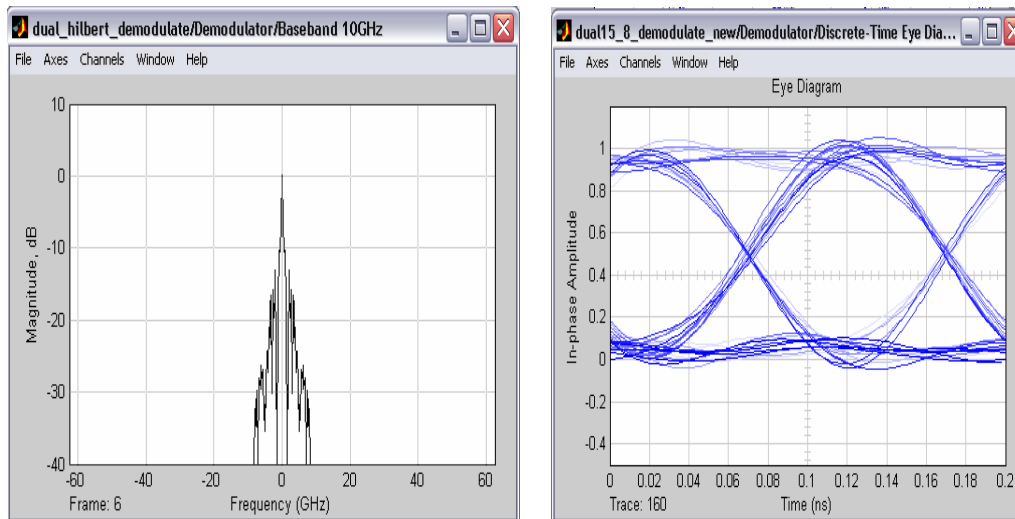


(a)

(b)

(c)

Figure 52: Demodulate f_c carrier time scope (b) Demodulate cosine signal time scope before LPF(c) Demodulate signal time scope after LPF.



(a)

(b)

Figure 53: (a) Demodulated signal spectrum and (b) Demodulated signal Eye Diagram has $Q = 8$ and $BER = 10^{-15}$ - hence complete error free.

6 Concluding Remarks and Further Development

6.1 Further Development

In this works, there are a lot of modulation formats that have not been developed such as RZ-CS SSB, OFDM modulation. Receivers of the optical communication system also have not been designed at this stage.

The optical receiver (Figure 54) is integrated from photo-detector, preamplifier, equalizer, filter and data recovery circuit. The photo-detector is detected the light signal and converts the light into the electrical signal and transmit to another parts of the receiver. The signal is weak, so a preamplifier is required to amplify the signal in the receiver. However, the pre-amplifier cannot handle the high data rate signals because it has not enough bandwidth. Therefore, the equalizer is required to restore the required bandwidth. Filter is used to filter out the unwanted high frequency components [5]. The receiver has to be designed optimization of the output SNR, so that the sensitivity of the receiver that is very important factor when designing receiver model.

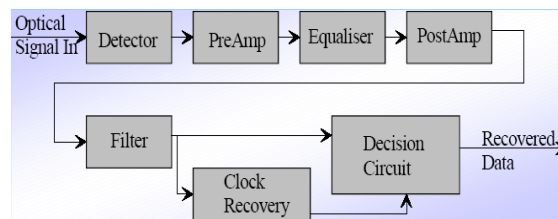


Figure 54: The block diagram of receiver [2]

6.2 Remarks

By using the SIMULINK platform a simulator has been developed. It is easier and much simpler for understanding the signal flow of an optical communication system. Unlike photonic hardware test-bed, the principal advantage of Simulink is that lightwaves can be illustrated for examination at each path of the optical flow.

Each sub-system involves different digital signal processing techniques and the model has successfully structured the simulator. The optical carrier that is transmitted through

the MZIM has been thoroughly represented and monitored. Standard analog and digital modulation techniques are applied. Shape pulsing, pulse modulation, ASK modulation, SSB or DSB modulation, multiplexing, de-multiplexing, demodulation etc. are well presented in the Simulink platform.

This work focuses on the modulation format generated at the output of the optical transmitter of advanced optical communication systems. We have demonstrated the optical spectra and eye diagrams of different modulation formats for RZ and NRZ with Gaussian and raised cosine pulse profiles. Optical multiplexers and de-multiplexers have been developed and tested for 16 or 32 channels with 100 GHz, 200 GHz channel spacing. Single and dual electrode driven MZIM for generation of optical DSB and SSB formats have been developed. These optical formats have been demonstrated in experimental systems.

Finally, the developed simulation models are partially integrated with other Simulink models of the SOATS series to propagate and amplify the signal to simulate a complete optically amplified and dispersion managed DWDM optical communication systems.

7 References

- [1] G. P. Agrawal *Fiber-optic Communication Systems*, 2nd ed. N.Y.: Academic Press, 2002.
- [2] L. N. Binh, and Z. Csematomy;
- [3] W. Tomasi, *Electronic Communication Systems Fundamentals*, 3rd ed: Prentice Hall.
- [4] K.-P. Ho, "Raised Cosine function in time domain as defined "Spectrum of externally modulated optical signals," *IEEE J. Lighjtw. Tech.*, 2004.
- [5] J. Hecht, *Understanding Fiber Optics*: Prentice Hall, 1997.
- [6] G. N. Smith, D; and Z. Ahmed, ""Overcoming Chromatic-dispersion Effects in Fiber-Wireless Systems Incorporating External Modulators"," *IEEE Trans. Microwave Th. and Tech.*, vol. 45, 1997.
- [7] B. P. Lathi, *Modern Digital and Analog Communications Systems*. Oxford: Oxford University Press, 1998.

8 Appendix

8.1 Simulation Requirement

8-52

In order to ensure that this simulation system operates at the best optimal performance it is recommended to be running on MatLab 6.5.1 or 7 R14 and above because the SIMULINK Blockset problems that are fully solved using this version.

In this model part, the following Simulink libraries are used: the *DSP Blockset* and *Communication Blockset*. For the S-function Block, a C program and MATLAB .m file is included.

8.2 Initialization

The SIMULINK simulator is to be open in Simulink Matlab and initialized the system parameters using the *initialize.m* file. Then open the SIMULINK.mdl file. The directory path in this file can be commented or changed the directory path to where the file is saved. This is a simple initialization file. It contains all parameters specified for the sub-systems, e.g. the data rate of the data input signal which is 10 Gb/s in this report. For future development, it is easier to change the data input rate to 40 Gb/s or above.

8.3 Simulation Block Specification

8.3.1 FFT Spectrum Scope

The buffer size setting is set according to the sampling time. The buffer size (Figure 55) should be larger than sampling one symbol frame size. It is set at 2 to power of x. The Spectrum scope can be defined as:

$$SpectrumFFT = \frac{1}{X} \sum_{X=1}^{X=N} S(t) \dots\dots\dots(24)$$

If the buffer FFT is used, this spectrum scope has a problem on power displaying. It has to multiply a signal by 1/X before the signal is sent into the spectrum scope.

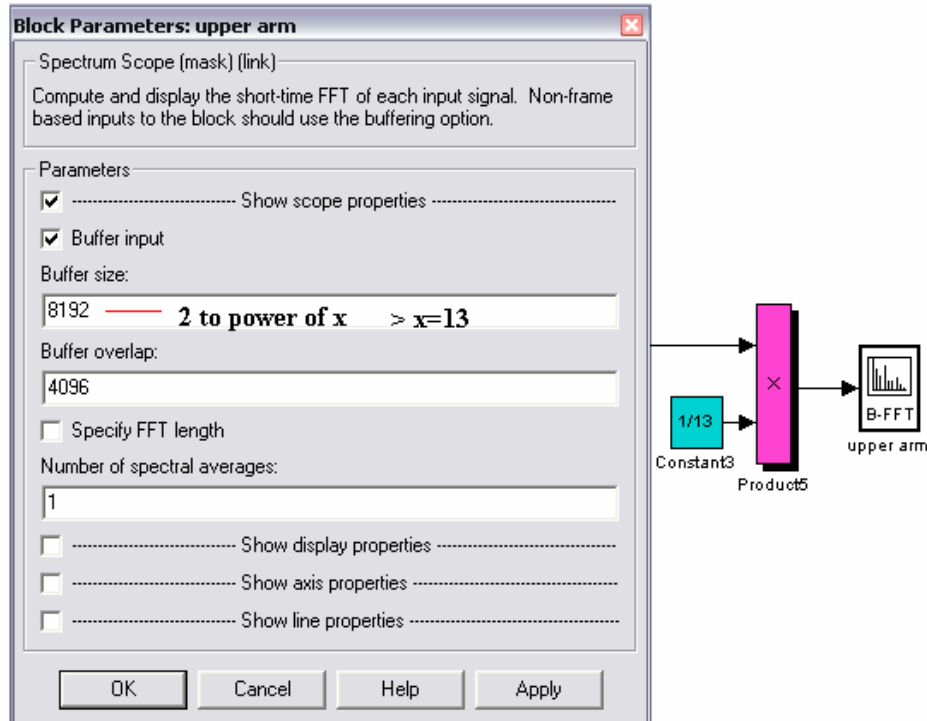


Figure 55 Spectrum Scope Specification

8.3.2 Zero-Order Hold

This block is used for setting the signal input as continuous wave. Note that some of the displaying scope of the SIMULINK accepts only discretized signals and the sample time is the system sampling time. The system must have one consistent sampling time which can be specified by the Nyquist frequency F_s which is at least *twice* the highest frequency in the system. The higher the sampling rate F_s the more accurate the processing would be.

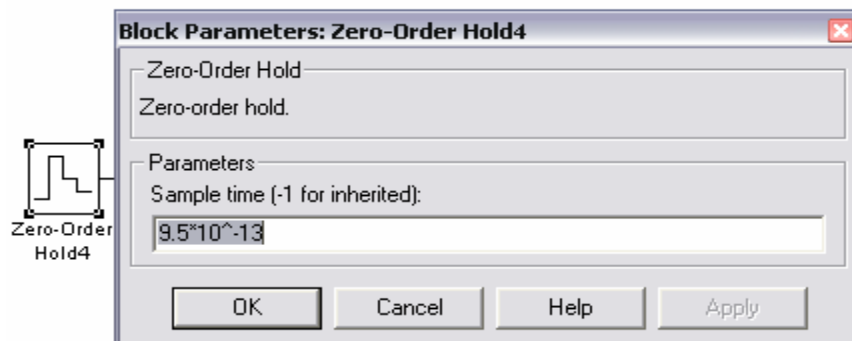


Figure 56: Zero-Hold Order Specification

8.3.3 Phase Modulation

This is Phase Modulation block. The phase modulation can be defined as:

$$\cos(2\pi f_c t + K_c u(t) + \theta) \quad (25)$$

where $u(t)$ is the modulating signal, K_c is the optical modulation index and θ is initial phase in radians that is controlled by the normalized *bias voltage* applied to MZIM. The Carrier Frequency is the frequency of the modulated carrier signal.

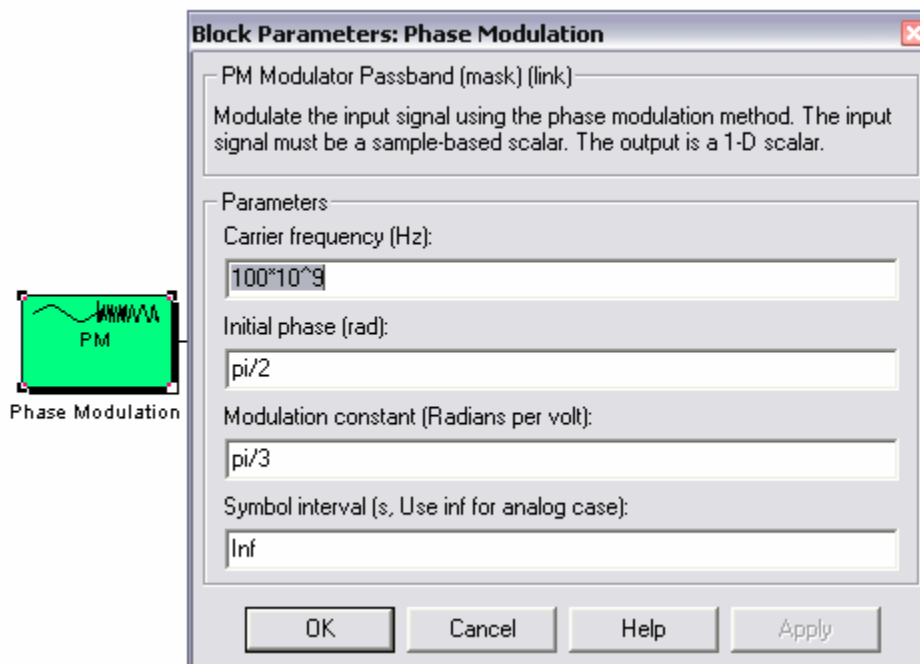


Figure 57 Phase Modulation block specification

8.3.4 S-Function

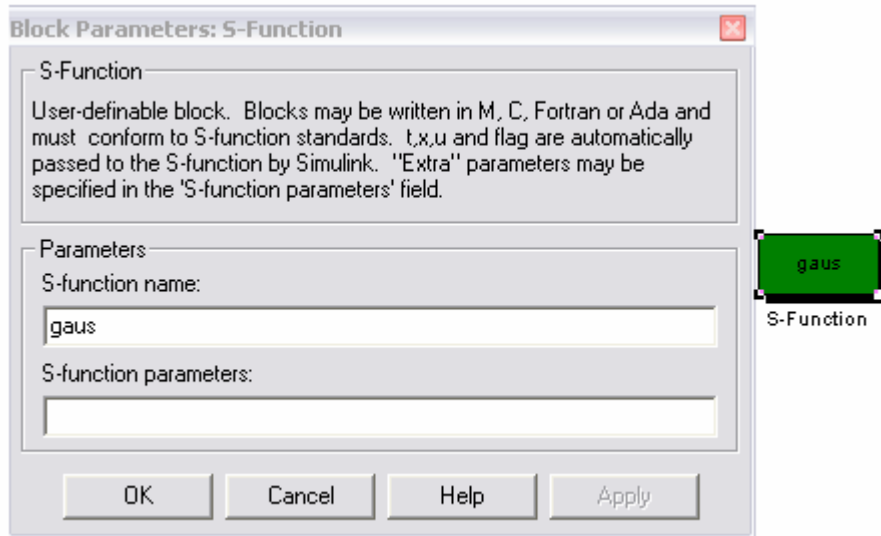
The following is the main part of the *gauss.m* S-function block setting. This SIMULINK blocks accept in time domain signal, so that if the signal that you want to display in frequency domain that is required FFT Block.

Gauss.m


```

function [sys,x0,str,ts] = gaus(t,x,u,flag)
%=====
% Function mdl Outputs performing the calculations.
%=====
function sys = mdlOutputs(t,x,u)
sys = exp(-(u/.35)^2);
% End of mdlOutputs.

```



8.3.5 Digital Filter Design

This filter block has different types of filters, such as LPF, High Pass Filter and Bandpass Filter etc. Frequency Specification is the range of the frequencies that the SIMULINK design model is needed. F_s is the system sampling frequency.

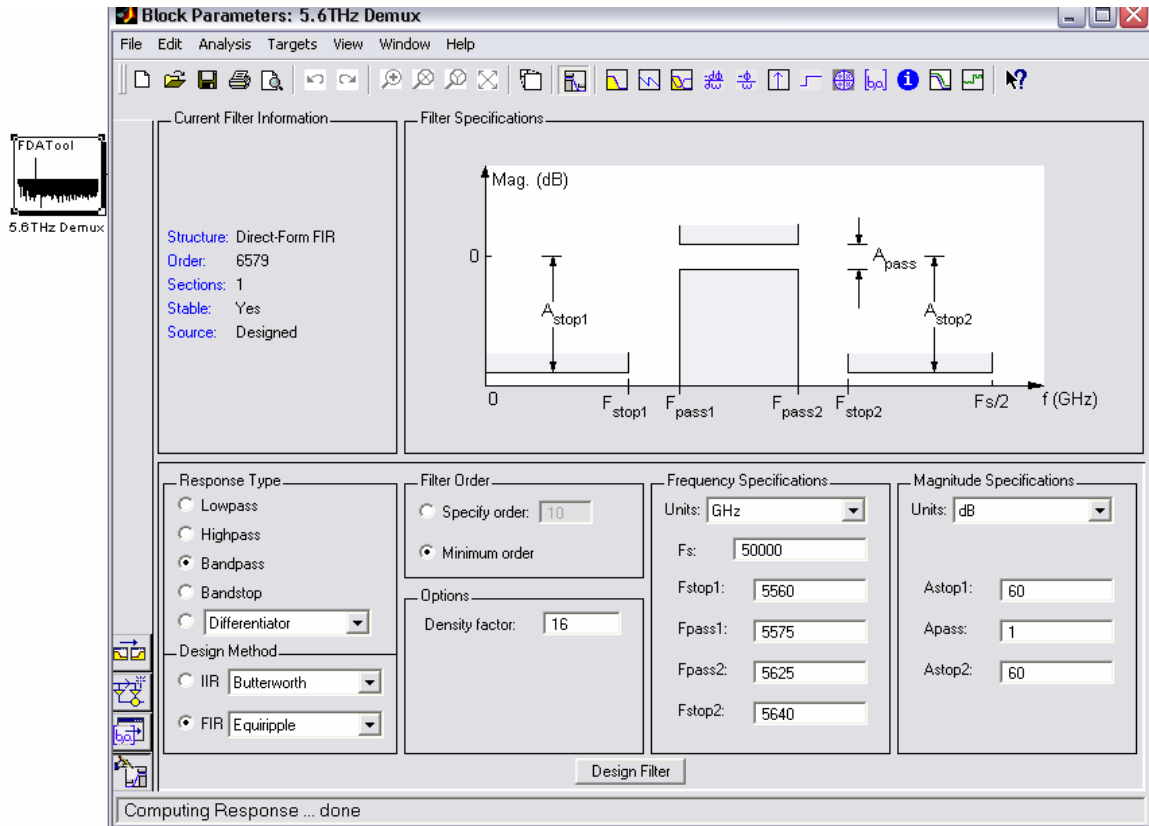


Figure 58: Digital Filter Specification

8.3.6 Time Eye Diagram Scope

This eye diagram Samples per symbol is according to the system sampling frequency and signal frequency. The sample per symbol is indicated as each symbol signal that is required how many times to sample it. It can be defined as:

$$\text{Samples_per_symbol} = \frac{F_s}{F_{data}} \quad (26)$$

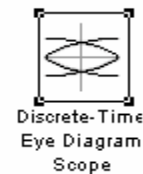
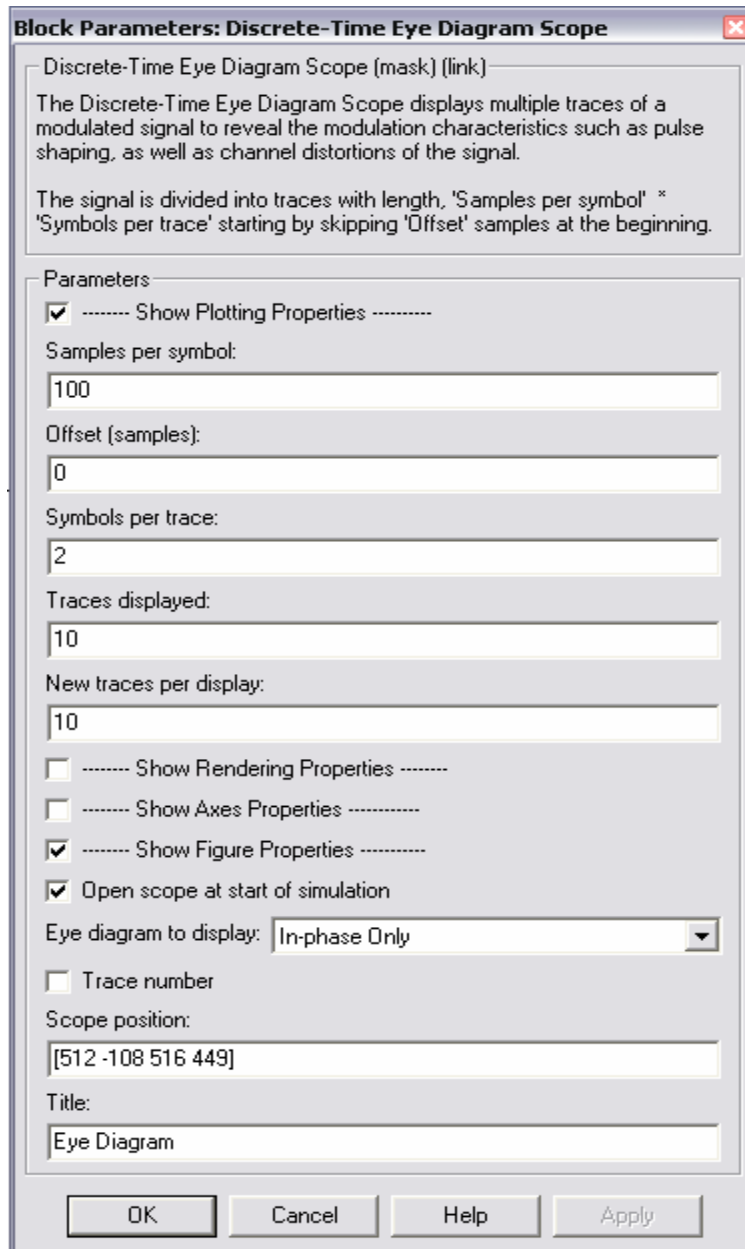


Figure 59 Eye diagram specification

<i>Channel labels</i>	<i>Carrier Frequency (THz)</i>	<i>Wavelength (nm)</i>	<i>Scaled Frequencies(THz)</i>
<i>fc1</i>	191.9	1560.23	5.5
<i>fc2</i>	192	1561.42	5.6
<i>fc3</i>	192.1	1560.61	5.7
<i>fc4</i>	192.2	1559.79	5.8
<i>fc5</i>	192.3	1558.98	5.9
<i>fc6</i>	192.4	1558.17	6
<i>fc7</i>	192.5	1557.36	6.1
<i>fc8</i>	192.6	1556.55	6.2
<i>fc9</i>	192.7	1555.75	6.3
<i>fc10</i>	192.8	1554.94	6.4
<i>fc11</i>	192.9	1554.13	6.5
<i>fc12</i>	193	1553.33	6.6
<i>fc13</i>	193.1	1552.52	6.7
<i>fc14</i>	193.2	1551.72	6.8
<i>fc15</i>	193.3	1550.92	6.9
<i>fc16</i>	193.4	1550.12	7
<i>fc17</i>	193.5	1549.32	7.1
<i>fc18</i>	193.6	1548.51	7.2
<i>fc19</i>	193.7	1547.72	7.3
<i>fc20</i>	193.8	1546.92	7.4
<i>fc21</i>	193.9	1546.12	7.5
<i>fc22</i>	194	1545.32	7.6
<i>fc23</i>	194.1	1544.53	7.7
<i>fc24</i>	194.2	1543.73	7.8
<i>fc25</i>	194.3	1542.94	7.9
<i>fc26</i>	194.4	1542.14	8
<i>fc27</i>	194.5	1541.35	8.1
<i>fc28</i>	194.6	1540.56	8.2
<i>fc29</i>	194.7	1539.77	8.3
<i>fc30</i>	194.8	1538.98	8.4
<i>fc31</i>	194.9	1538.19	8.5
<i>fc32</i>	195	1537.4	8.6

Table 2: *ITU-T standard frequency allocation for 100 GHz C-band and their scaled counterparts.*